UNIVERSIDADE FEDERAL DE MINAS GERAIS
INSTITUTO DE CIÊNCIAS BIOLÓGICAS
DEPARTAMENTO DE BIOLOGIA GERAL
PROGRAMA DE PÓS-GRADUAÇÃO EM GENÉTICA

DISSERTAÇÃO DE MESTRADO

ESTRUTURA GENÉTICA, DINÂMICA POPULACIONAL E DEMOGRAFIA HISTÓRICA DO TAMANDUÁ-BANDEIRA *Myrmecophaga tridactyla* LINNAEUS, 1758 (PILOSA: MYRMECOPHAGIDAE)

AUTOR: Raphael Teodoro Franciscani Coimbra

ORIENTADOR: Prof. Dr. Fabrício Rodrigues dos Santos

BELO HORIZONTE

Agosto - 2017

UNIVERSIDADE FEDERAL DE MINAS GERAIS

INSTITUTO DE CIÊNCIAS BIOLÓGICAS

DEPARTAMENTO DE BIOLOGIA GERAL

PROGRAMA DE PÓS-GRADUAÇÃO EM GENÉTICA

RAPHAEL TEODORO FRANCISCANI COIMBRA

ESTRUTURA GENÉTICA, DINÂMICA POPULACIONAL E DEMOGRAFIA HISTÓRICA DO TAMANDUÁ-BANDEIRA *Myrmecophaga tridactyla* LINNAEUS, 1758 (PILOSA: MYRMECOPHAGIDAE)

Dissertação apresentada como requisito parcial para a obtenção do grau de Mestre em Genética pelo programa de Pós-Graduação em Genética, Departamento de Biologia Geral, Instituto de Ciências Biológicas, Universidade Federal de Minas Gerais.

Orientador: Prof. Dr. Fabrício Rodrigues dos Santos

Belo Horizonte

Agosto - 2017

043 Coimbra, Raphael Teodoro Franciscani.
Estrutura genética, dinâmica populacional e demografia histórica do tamanduá-bandeira *Myrmecophaga tridactyla* Linnaeus, 1758 (Pilosa: Myrmecophagidae) [manuscrito] / Raphael Teodoro Franciscani Coimbra. – 2017.

63 f. : il. ; 29,5 cm.

Orientador: Prof. Dr. Fabrício Rodrigues dos Santos.
Dissertação (mestrado) – Universidade Federal de Minas Gerais, Instituto de Ciências Biológicas.

1. Genética. 2. Filogeografia. 3. Dinâmica populacional. 4. Tamanduá-bandeira. 5. Fluxo gênico. I. Santos, Fabrício Rodrigues dos. II. Universidade Federal de Minas Gerais. Instituto de Ciências Biológicas. III. Título.

CDU: 575

Ficha catalográfica elaborada pela Biblioteca do Instituto de Ciências Biológicas da UFMG

Pós-Graduação em Genética
Departamento de Biologia Geral, ICB
Universidade Federal de Minas Gerais
Av. Antônio Carlos, 6627 - C.P. 486 - Pampulha - 31270-901 - Belo Horizonte - MG
e-mail: pg-gen@icb.ufmg.br FAX: (+31) - 3409-2570

"Estrutura genética, dinâmica populacional e demografia histórica do tamanduá-bandeira Myrmecophaga tridactyla Linnaeus, 1758 (Pilosa: Myrmecophagidae)"

Raphael Teodoro Franciscani Coimbra

Dissertação aprovada pela banca examinadora constituída pelos Professores:

Fabrício Rodrigues dos Santos
UFMG

Gustavo Campos e Silva Kuhn
UFMG

Ubirajara de Oliveira
UFMG

Belo Horizonte, 25 de agosto de 2017.

Aos meus pais e à Mel, que me incentivaram a tentar e me ajudaram a não desistir.

AGRADECIMENTOS

Agradeço ao Prof. Fabrício R. Santos a oportunidade e orientação durante os cinco anos em que fiz parte do LBEM.

Agradeço também ao Rafael e ao José Eustáquio a valiosa ajuda no momento em que mais precisei.

Aos colegas do LBEM, obrigado pela troca de ideias e de experiências.

Aos meus amigos Marco e Samuel, muito obrigado pelas discussões construtivas, conversas de todos os tipos e risadas, muitas risadas.

A todos que forneceram amostras para a execução deste trabalho, José Eustáquio, Arnaud Desbiez, Carmen Ruiz, Pedro Galetti, Ana Luiza Queiroz, Evanguedes Kalapothakis, Fernanda Braga e Museu de História Natural Capão da Imbuia, meus sinceros agradecimentos.

Muito obrigado, especialmente, à minha família e a Mel pelo apoio e a compreensão. Vocês foram a minha motivação durante os momentos de desânimo.

ÍNDICE

LISTA DE FIGURAS

INTRODUÇÃO

CAPÍTULO I

LISTA DE TABELAS

CAPÍTULO I

LISTA DE ABREVIATURAS

[AM] = população da Amazônia

[CEPTAF] = população do Cerrado, Pantanal e Mata Atlântica

°C = graus Celsius

AF = Mata Atlântica

AM = Amazônia

AMOVA = análise de variância molecular

BDNF = fator neurotrófico derivado do cérebro

BSA = albumina sérica bovina

ca. = cerca de

CE = Cerrado

CI = intervalo de confiança

CITES = Convenção sobre o Comércio Internacional das Espécies da Flora e da Fauna Selvagens Ameaçadas de Extinção

Cytb = citocromo b

DNA = ácido desoxirribonucléico

dNTPs = desoxirribonucleotídeos trifosfatados

EBSP = extended Bayesian skyline plot

ESS = tamanho amostral efetivo

h = diversidade haplotípica

HVI = região hipervariável I

IPs = reservas de proteção integral

IUCN = União Internacional para a Conservação da Natureza

K = número de populações

kya = milhares de anos atrás

LBEM = Laboratório de Biodiversidade e Evolução Molecular

M = taxa de imigração efetiva escalada pela mutação

m = taxa de imigração

MCMC = Markov Chain Monte Carlo

mg = miligrama

min = minutos

mL = mililitro

mM = milimolar

MMA = Ministério do Meio Ambiente

mtDNA = DNA mitocondrial

mya = milhões de anos atrás

nDNA = DNA nuclear

N_e = tamanho efetivo populacional

ng = nanograma

N_m = número efetivo de migrantes por geração

P = probabilidade

pb e bp = pares de base

PAs = áreas protegidas

PCR = reação em cadeia da polimerase

PT = Pantanal

R_{mtDNA} = razão transição/transversão do DNA mitocondrial

R/E = rarefação/extrapolação

RAG2 = gene ativador da recombinação 2

s = segundos

SUs = reservas de uso sustentável

$tRNA^{Pro}$ = ácido ribonucleico transportador de prolina

$tRNA^{Thr}$ = ácido ribonucleico transportador de treonina

U = unidades

UFMG = Universidade Federal de Minas Gerais

vWF = exon 28 do fator de von Willebrand

Θ = tamanho efetivo populacional escalado pela mutação

μ = taxa de mutação

μL = microlitro

μM = micromolar

π = diversidade nucleotídica

τ = tempo de geração

φ_{ST} = análogo molecular do índice de fixação

RESUMO

O tamanduá-bandeira (*Myrmecophaga tridactyla* Linnaeus, 1758) é a maior dentre as espécies atuais tamanduás e se distribui desde Honduras até o norte da Argentina, habitando desde florestas úmidas e decíduas até savanas e campos abertos. A espécie é constantemente ameaçada pela caça ilegal, perda e fragmentação de habitat, fogo e atropelamentos em estradas, e sofre com o declínio populacional. Atualmente, está possivelmente extinta em Belize, El Salvador, Guatemala e Uruguai. Dessa forma, *M. tridactyla* é classificado como vulnerável pela IUCN e integra o Apêndice II da CITES. No Brasil, o tamanduá-bandeira está possivelmente extinto nos estados do Rio Grande do Sul, Santa Catarina, Rio de Janeiro e Espírito Santo. Além disso, poucas áreas abrigam populações grandes da espécie, como os Parques Nacionais das Emas e da Serra da Canastra, ambos localizados no Cerrado. Entretanto, esse bioma é ameaçado pela expansão das fronteiras agropecuárias e a produção de carvão vegetal. Assim, *M. tridactyla* também é classificado como vulnerável pelo Ministério do Meio Ambiente. Uma pesquisa anterior com populações brasileiras de tamanduá-bandeira mostrou evidências de estruturação e expansão populacional. Neste estudo, avaliamos os padrões geográficos da diversidade genética, a dinâmica de fluxo gênico e alterações demográficas históricas em populações da espécie no Brasil. Analisamos 2854 pb de sequências mitocondriais e nucleares de 106 indivíduos provenientes do Cerrado (CE), Pantanal (PT), Amazônia (AM) e Mata Atlântica (AF). Construímos redes de haplótipos, realizamos análises de agrupamento bayesiano e de variância molecular, e calculamos as diversidades haplotípica e nucleotídica. Além disso, fizemos curvas de rarefação/extrapolação de riqueza de haplótipos, seleção de modelos de migração e reconstrução demográfica. A análise do DNA mitocondrial confirmou a existência de dois grupos genéticos distintos (φ_{ST} = 0.3275): um na AM, grupo [AM]; e outro nos biomas CE, PT e AF, grupo [CEPTAF]. A diversidade haplotípica mitocondrial observada para *M. tridactyla* (h = 0.7623) foi moderada se comparada a outras espécies ameaçadas e não-ameaçadas. Ao nível populacional, a riqueza de haplótipos mitocondriais tende a ser maior em [CEPTAF] do que em [AM], provavelmente, devido a esta última apresentar um menor tamanho populacional efetivo. Encontramos fluxo gênico de [AM] para [CEPTAF], possivelmente, devido a maior disponibilidade de alimentos e a preferência de *M. tridactyla* por habitats heterogêneos presentes no CE e PT. Também detectamos um crescimento populacional de ~ 7.5 vezes nos últimos 60 mil anos e discutimos hipóteses sobre suas causas. Em conclusão, mostramos a influência de características ecológicas de *M. tridactyla* sobre a história natural e a configuração da diversidade genética de suas populações, reforçando a importância do CE para a conservação da espécie.

ABSTRACT

The giant anteater (*Myrmecophaga tridactyla* Linnaeus, 1758) is the largest of all current anteater species and ranges from Honduras to northern Argentina, inhabiting from moist and deciduous forests to savannas and grasslands. The species is constantly threatened by poaching, habitat loss and fragmentation, wildfires and road kills, and its population numbers are declining. Currently, it is likely extinct in Belize, El Salvador, Guatemala and Uruguay. Therefore, *M. tridatyla* is listed as vulnerable by IUCN and integrates the CITES Appendix II. In Brazil, the giant anteater is possibly extinct in the states of Rio Grande do Sul, Santa Catarina, Rio de Janeiro and Espírito Santo. Additionally, a few areas harbor large populations of the species, such as the Emas and the Serra da Canastra National Parks, both located in the Cerrado. However, this biome is threatened by the expansion of agricultural lands, livestock and production of charcoal. Hence, the Brazilian Ministry of Environment also lists *M. tridactyla* as vulnerable. A previous study on Brazilian populations of giant anteaters found evidences of both population structure and expansion. Here, we investigate the geographic patterns of genetic diversity, gene flow dynamics and historical population size changes in the species' populations in Brazil. We analyzed 2854 bp of mitochondrial and nuclear sequences of 106 individuals from Cerrado (CE), Pantanal (PT), and both Amazon (AM) and Atlantic Forests (AF). We constructed haplotype networks, performed both a Bayesian clustering analysis and an analysis of molecular variance, and calculated the haplotype and nucleotide diversities. Furthermore, we estimated rarefied/extrapolated haplotype richness curves and carried out both migration model selection and demographic reconstruction. The analysis of mitochondrial DNA confirmed the existence of two distinct genetic clusters (φ_{ST} = 0.3275): one in the AM biome, cluster [AM]; and another in the CE, PT and AF biomes, cluster [CEPTAF]. The mitochondrial haplotype diversity observed for the species (h = 0.7623) was moderate when compared to other threatened and non-threatened species. At the population level, the mitochondrial haplotype richness showed a trend to be higher in [CEPTAF] than in [AM], probably due to a smaller effective population size for the latter. We found gene flow from [AM] to [CEPTAF], possibly due to both greater food availability and *M. tridactyla*'s preference for heterogeneous habitats found in both CE and PT. We also recovered a ~ 7.5-fold increase in population size since 60 kya and discussed hypotheses for its causes. In conclusion, we demonstrated the influence of ecological characteristics of *M. tridactyla* on both the natural history and genetic diversity configuration of its populations, reinforcing the importance of the CE for the species' conservation.

INTRODUÇÃO

A magnordem Xenarthra Cope, 1889 é endêmica do continente americano e considerada uma das principais linhagens de mamíferos placentários (Madsen et al., 2001; Murphy et al., 2001; Delsuc et al., 2002; Meredith et al., 2011). As espécies de xenartros são classificadas em duas ordens: Cingulata (tatus) e Pilosa (tamanduás e preguiças; Gardner, 2007). Dentro da ordem Pilosa, os tamanduás (Vermilingua) formam uma subordem própria que se diferencia das preguiças (Folivora), dentre outras características, pela completa ausência de dentes e presença de uma língua longa, protrátil e vermiforme (Gardner, 2007). Das quatro espécies de vermilinguas atuais, três são classificadas na família Myrmecophagidae (Gardner, 2007). Estão incluídos nesta família dois gêneros que divergiram durante o Mioceno Médio: *Myrmecophaga* e *Tamandua* (Delsuc, Vizcaíno & Douzery, 2004; Delsuc et al., 2001; 2012; Gibb et al., 2016). O tamanduá-bandeira, *Myrmecophaga tridactyla* Linnaeus, 1758 (Figura 1), é o único representante de seu gênero e a maior dentre todas as espécies de tamanduás, com adultos atingindo em média 2 m de comprimento e pesando 33 kg (Gardner, 2007). A espécie pode ser encontrada em diversos tipos de habitats, desde florestas úmidas e decíduas até savanas e campos abertos (Wetzel, 1982; Medri, Mourão & Rodrigues, 2011). Nesses ambientes, apresenta atividade diurna e/ou noturna de acordo com as condições de temperatura (Camilo-Alves & Mourão, 2006; Desbiez & Medri, 2010; Di Blanco, Spørring & Di Bitetti, 2016) e se alimenta de formigas e cupins (Montgomery, 1985; Medri, Mourão & Harada, 2003; Sandoval-Gómez, Ramírez-Chaves & Marín, 2012; Braga et al., 2014). Os indivíduos costumam ser solitários, exceto durante os períodos de acasalamento e de cuidado parental materno (Shaw, Machado-Neto & Carter, 1987). Os tamanduás-bandeiras se reproduzem ao longo do ano e as fêmeas dão à luz um único filhote, após cerca de 171 a 184 dias de gestação, do qual cuidarão por aproximadamente seis a oito meses (Patzl et al., 1998; Knott et al., 2013).

Figura 1. Tamanduá-bandeira (*Myrmecophaga tridactyla* Linnaeus, 1758) caminhando pelo Cerrado. Créditos de imagem para © Stephan Bonneau/Biosphoto.

Atualmente, *M. tridactyla* se distribui desde Honduras, na América Central, até a região do Gran Chaco da Bolívia, Paraguai e norte da Argentina, e está possivelmente extinto em Belize, El Salvador, Guatemala e Uruguai (Figura 2; Miranda, Bertassoni & Abba, 2014). Em grande parte de sua distribuição, o tamanduá-bandeira é constantemente ameaçado pela caça ilegal (Leeuwenberg, 1997; Noss, Cuéllar & Cuéllar, 2008; Meritt, 2008), perda e fragmentação de habitat (Harris et al., 2005; Klink & Machado, 2005; Ribeiro et al., 2009), fogo (Silveira et al., 1999) e atropelamentos em estradas (Cáceres et al., 2010; Cunha, Moreira & Silva, 2010; Freitas, Justino & Setz, 2014). Por isso, estima-se uma perda de pelo menos 30% da população nos últimos 10 anos (Miranda et al., 2014). Devido às reais ameaças e ao perceptível declínio populacional, a União Internacional para a Conservação da Natureza (sigla em inglês, IUCN) classifica *M. tridactyla* na categoria Vulnerável em sua lista vermelha (IUCN, 2016). Da mesma forma, a Convenção sobre o Comércio Internacional das Espécies da Flora e da Fauna Selvagens Ameaçadas de Extinção (sigla em inglês, CITES) lista o tamanduá-bandeira em seu Apêndice II (CITES, 2017). No Brasil, a espécie está possivelmente extinta nos estados do Rio Grande do Sul, Santa Catarina, Rio de Janeiro e Espírito Santo (Figura 2; Miranda et al., 2014). Além disso, poucas áreas abrigam populações grandes do animal, como o Parque Nacional das Emas (Miranda et al., 2006) e o Parque Nacional da Serra da Canastra (Shaw et al., 1987), ambos localizados no Cerrado brasileiro.

Entretanto, esse bioma se encontra cada vez mais ameaçado pela expansão das fronteiras agropecuárias para a produção de soja, milho, arroz, a formação de pastagens para criação de gado e a produção de carvão vegetal (Ratter, Ribeiro & Bridgewater, 1997; Klink & Machado, 2005). Assim, devido ao declínio no tamanho das populações associado à perda de habitat, *M. tridactyla* também está incluído na lista oficial de espécies da fauna ameaçadas de extinção, elaborada pelo Ministério do Meio Ambiente (MMA), na categoria Vulnerável (MMA, 2014).

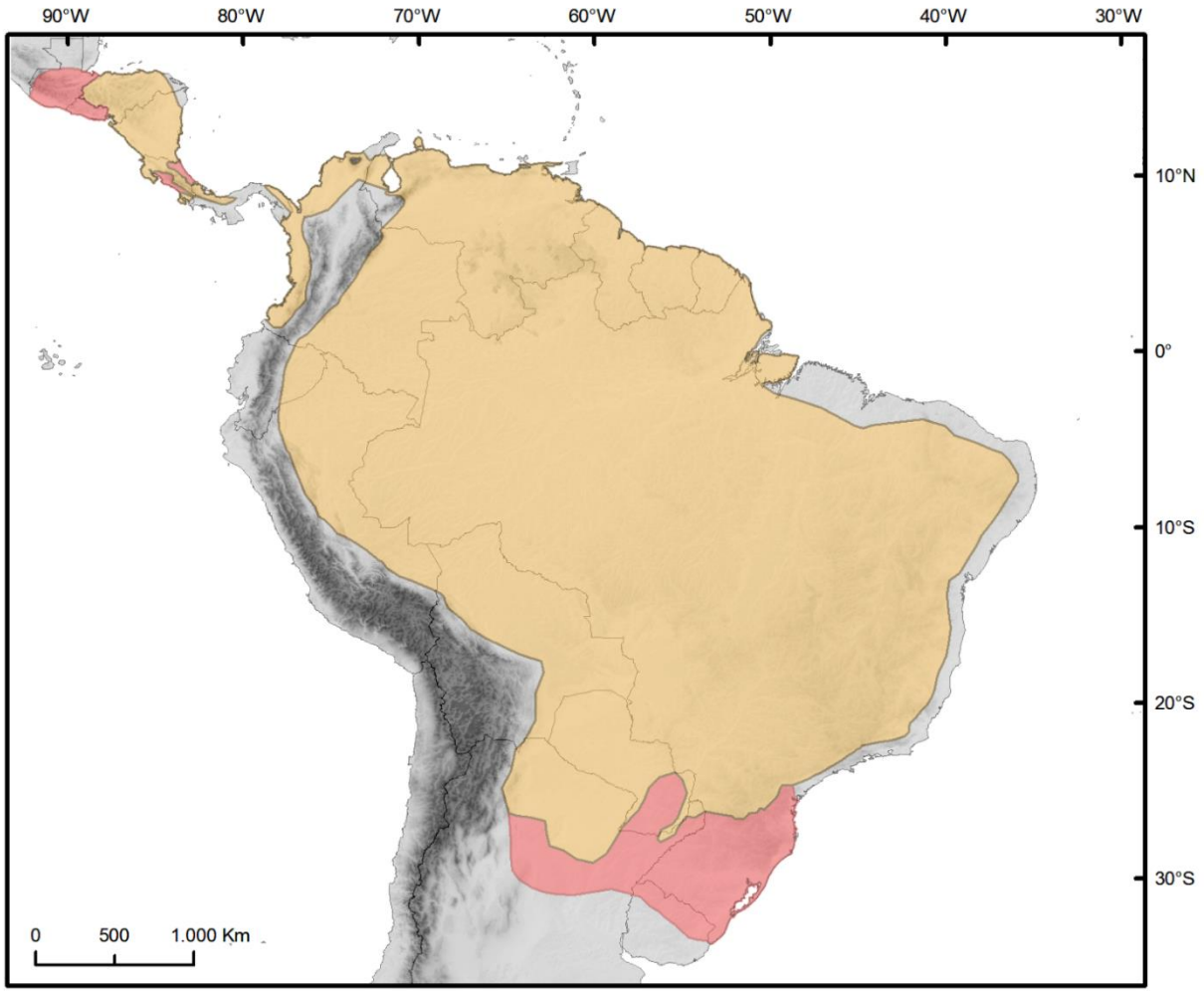

Figura 2. Distribuição geográfica atual (em amarelo) e histórica (em vermelho) de *Myrmecophaga tridactyla* Linnaeus, 1758. Mapa produzido com ArcGIS v10.4 e dados da IUCN (2016).

A dieta especializada, a baixa taxa reprodutiva, a dificuldade de criação e reprodução em cativeiro (Superina, Miranda & Plese, 2008; Leiva e Marques, 2010), incluindo problemas de saúde nos animais (Diniz, Costa & Oliveira, 1995; Morford & Meyers, 2003), são características intrínsecas de *M. tridactyla* que facilitam seu declínio. Somados às ameaças antrópicas, esses fatores evidenciam a necessidade de monitoramento populacional e

investimentos na sua conservação. Para tanto, além de pesquisas sobre a biologia e ecologia de *M. tridactyla*, é essencial conhecer a estrutura genética de suas populações. Assim, será possível identificar populações de interesse, definir unidades de manejo, identificar populações e locais para reintrodução e aprimorar o entendimento sobre a história natural da espécie (Frankham, Ballou & Briscoe, 2010). Porém, apesar de considerado um dos xenartros mais icônicos, o tamanduá-bandeira apresenta um repertório muito restrito de estudos genéticos intraespecíficos a seu favor. Hsu (1965) e Pereira Júnior, Jorge & Costa (2004) descreveram o cariótipo da espécie (2n = 60 XX/XY) utilizando técnicas de coloração cromossômica convencionais em poucos indivíduos de cativeiro. Rossi et al. (2014) fizeram uma caracterização citogenética completa de *M. tridactyla* em 26 espécimes ao longo de sua distribuição na Argentina, incluindo bandeamentos G e C, coloração de regiões organizadoras do nucléolo, hibridização fluorescente *in situ* e análise do complexo sinaptonêmico. Garcia et al. (2005) isolaram e caracterizaram seis marcadores microssatélites para a espécie, dos quais cinco foram utilizados por Colevatti et al. (2007) para estudar as populações do Parque Nacional das Emas, onde encontraram baixos níveis de polimorfismo em todos os *loci* e elevado coeficiente de endogamia. Clozato et al. (2017) foram os primeiros a estudar, em escala nacional, a filogeografia das populações de tamanduá-bandeira de Cerrado, Pantanal, Amazônia e Mata Atlântica, incluindo amostras dos Parques Nacionais das Emas e da Serra da Canastra. Através do uso de marcadores mitocondriais e nucleares, os autores avaliaram a diversidade genética e os padrões filogeográficos na espécie. Seus resultados evidenciaram pouca diferenciação entre indivíduos do Cerrado e Pantanal, a existência de uma barreira para o fluxo gênico entre essas populações e aquelas da Amazônia e uma possível conexão passada entre Mata Atlântica e Amazônia. Além disso, os autores encontraram uma maior diversidade genética e sinais de expansão demográfica nas populações de Cerrado, principalmente nos Parques Nacionais, indicando que tais populações serviriam como redutos de diversidade para a espécie.

Apesar de, nas palavras de Aguiar & Fonseca (2008), os xenartros representarem “uma concentração única de história evolutiva no continente americano”, a maioria das espécies do grupo permanece inadequadamente estudada. Infelizmente, esta afirmação se sustenta também para o tamanduá-bandeira (Diniz & Brito, 2012). Dessa forma, visando construir um cenário mais completo da história evolutiva e da diversidade de *M. tridactyla*, este projeto dá continuidade aos estudos iniciados por Clozato et al. (2017) aumentando seu alcance geográfico, com a obtenção de novas amostras, e sua potencial aplicação para a conservação, através da utilização de diferentes marcadores moleculares e de análises mais aprofundadas da demografia histórica e dinâmica populacional da espécie.

REFERÊNCIAS

Aguiar JM, Fonseca GAB. 2008. Conservation status of the Xenarthra. Em: Vizcaino SF, Loughry WJ, eds. *The biology of the Xenarthra*. Gainesville, FL: University Press of Florida, 215-231.

Braga FG, Souza NJ, Batista AC, Lima PPS. 2014. Consumo de formigas cortadeiras por tamanduá-bandeira *Myrmecophaga tridactyla* (Linnaeus, 1758) em plantios de *Pinus* spp. no Paraná, Brasil. *Edentata* 15: 1-8.

Cáceres NC, Hannibal W, Freitas DR, Silva EL, Roman C, Casella J. 2010. Mammal occurrence and roadkill in two adjacent ecoregions (Atlantic Forest and Cerrado) in south-western Brazil. *Zoologia* 27: 709-717.

Camilo-Alves CSP, Mourão GM. 2006. Responses of a specialized insectivorous mammal (*Myrmecophaga tridactyla*) to variation in ambient temperature. *Biotropica* 38: 52-56.

CITES. 2017. The CITES Appendices I, II and III. Disponível em: https://www.cites.org.

Clozato CL, Miranda FR, Lara-Ruiz P, Collevatti RG, Santos FR. 2017. Population structure and genetic diversity of the giant anteater (*Myrmecophaga tridactyla*: Myrmecophagidae, Pilosa) in Brazil. *Genetics and Molecular Biology* 40: 50-60.

Collevatti RG, Leite KCE, Miranda GHB, Rodrigues FHG. 2007. Evidence of high inbreeding in a population of the endangered giant anteater, *Myrmecophaga tridactyla* (Myrmecophagidae), from Emas National Park, Brazil. *Genetics and Molecular Biology* 30: 112-120.

Cunha HF, Moreira FGA, Silva SS. 2010. Roadkill of wild vertebrates along the GO-060 road between Goiânia and Iporá, Goiás State, Brazil. *Acta Scientiarum. Biological Sciences*. 32: 257-263.

Delsuc F, Catzeflis FM, Stanhope MJ, Douzery EJP. 2001. The evolution of armadillos, anteaters and sloths depicted by nuclear and mitochondrial phylogenies: implications for the status of the enigmatic fossil *Eurotamandua*. *Proceedings of the Royal Society of London. Series B, Biological Sciences* 268: 1605-1615.

Delsuc F, Scally M, Madsen O, Stanhope MJ, de Jong WW, Catzeflis FM, Springer MS, Douzery EJP. 2002. Molecular phylogeny of living xenarthrans and the impact of character and taxon sampling on the placental tree rooting. *Molecular Biology and Evolution* 19: 1656-1671.

Delsuc F, Vizcaíno SF, Douzery EJP. 2004. Influence of Tertiary paleoenvironmental changes on the diversification of South American mammals: a relaxed molecular clock study within xenarthrans. *BMC Evolutionary Biology* 4(11).

Delsuc F, Superina M, Tilak M, Douzery EJP, Hassanin A. 2012. Molecular phylogenetics unveils the ancient evolutionary origins of the enigmatic fairy armadillos. *Molecular Phylogenetics and Evolution* 62: 673-680.

Desbiez ALJ, Medri IM. 2010. Density and habitat use by giant anteaters (*Myrmecophaga tridactyla*) and southern tamanduas (*Tamandua tetradactyla*) in the Pantanal wetland, Brazil. *Edentata* 11: 4-10.

Diniz MF, Brito D. 2012. The charismatic giant anteater (*Myrmecophaga tridactyla*): a famous John Doe? *Edentata* 13: 76-83.

Diniz LSM, Costa EO, Oliveira PMA. 1995. Clinical disorders observed in anteaters (Myrmecophagidae, Edentata) in captivity. *Veterinary Research Communications* 19: 409-415.

Di Blanco YE, Spørring KL, Di Bitetti MS. 2016. Daily activity pattern of reintroduced giant anteaters (*Myrmecophaga tridactyla*): effects of seasonality and experience. *Mammalia* 81: 11-21.

Frankham R, Ballou JD, Briscoe DA. 2010. *Introduction to conservation genetics*. 2nd edition. Cambridge, UK: Cambridge University Press.

Freitas CH, Justino CS, Setz EZF. 2014. Road-kills of the giant anteater in south-eastern Brazil: 10 years monitoring spatial and temporal determinants. *Wildlife Research* 41: 673-680.

Garcia JE, Vilas Boas LA, Lemos MVF, Lemos EGM, Contel EPB. 2005. Identification of microsatellite DNA markers for the giant anteater *Myrmecophaga tridactyla*. *Journal of Heredity* 96: 600-602.

Gardner AL. 2007. *Mammals of South America, volume 1: marsupials, xenarthrans, shrews, and bats*. Chicago, IL: University of Chicago Press.

Gibb GC, Condamine FL, Kuch M, Enk J, Moraes-Barros N, Superina M, Poinar HN, Delsuc F. 2016. Shotgun mitogenomics provides a reference phylogenetic framework and timescale for living xenarthrans. *Molecular Biology and Evolution* 33: 621-642.

Harris MB, Tomas W, Mourão G, Silva CJ, Guimarães E, Sonoda F, Fachim E. 2005. Safeguarding the Pantanal wetlands: threats and conservation initiatives. *Conservation Biology* 19: 714-720.

Hsu TC. 1965. Chromosomes of two species of anteaters. *Mammalian Chromosomes Newsletter* 15: 108-109.

IUCN. 2016. The IUCN red list of threatened species, version 2016-3. Disponível em: http://www.iucnredlist.org.

Klink CA, Machado RB. 2005. Conservation of the Brazilian Cerrado. *Conservation Biology* 19: 707-713.

Knott KK, Roberts BM, Maly MA, Vance CK, DeBeachaump J, Majors J, Riger P, DeCaluwe H, Kouba AJ. 2013. Fecal estrogen, progestagen and glucocorticoid metabolites during the estrous cycle and pregnancy in the giant anteater (*Myrmecophaga tridactyla*): evidence for delayed implantation. *Reproductive Biology and Endocrinology* 83: 1-13.

Leeuwenberg F. 1997 Edentata as a food resource: subsistence hunting by Xavante Indians, Brazil. *Edentata* 3: 4-5.

Leiva M, Marques MC. 2010. Dados reprodutivos da população cativa de tamanduá-bandeira (*Myrmecophaga tridactyla* Linnaeus, 1758) da Fundação Parque Zoológico de São Paulo. *Edentata* 11: 49-52.

Madsen O, Scally M, Douady CJ, Kao DJ, DeBry RW, Adkins R, Amrine HM, Stanhope MJ, de Jong WW, Springer MS. 2001. Parallel adaptive radiations in two major clades of placental mammals. *Nature* 409: 610-614.

Medri IM, Mourão GM, Harada AY. 2003. Dieta de tamanduá-bandeira (*Myrmecophaga tridactyla*) no Pantanal da Nhecolândia, Brasil. *Edentata* 5: 29-34.

Medri IM, Mourão GM, Rodrigues FHG. 2011. Ordem Pilosa. Em: Reis NR, Peracchi AL, Pedro WA, Lima IP, eds. *Mamíferos do Brasil*. 2ª edição. Londrina, PR: Reis NR, 91-106.

Meredith RW, Janečka JE, Gatesy J, Ryder OA, Fisher CA, Teeling EC, Goodbla A, Eizirik E, Simão TLL, Stadler T, Rabosky DL, Honeycutt RL, Flynn JJ, Ingram CM, Steiner C, Williams TL, Robinson TJ, Burk-Herrick A, Westerman M, Ayoub NA, Springer MS, Murphy WJ. 2011. Impacts of the Cretaceous terrestrial revolution and KPg extinction on mammal diversification. *Science* 334: 521-524.

Meritt DA. 2008. Xenarthrans of the Paraguayan Chaco. Em: Vizcaino SF, Loughry WJ, eds. *The biology of the Xenarthra*. Gainesville, FL: University Press of Florida, 294-299.

Miranda F, Bertassoni A, Abba AM. 2014. *Myrmecophaga tridactyla*. The IUCN red list of threatened species 2014: e.T14224A47441961.

Miranda GHB, Tomás WM, Valladares-Pádua CB, Rodrigues FHG. 2006. Giant anteater (*Myrmecophaga tridactyla*) population survey in Emas National Park, Brazil - a proposed monitoring program. *Endangered Species UPDATE* 23: 96-103.

MMA. 2014. Portaria nº 444/2014: lista nacional oficial de espécies da fauna ameaçadas de extinção. *Diário Oficial da União*.

Montgomery GG. 1985. Movements, foraging and food habits of the four extant species of neotropical vermilinguas (Mammalia; Myrmecophagidae). Em: Montgomery GG, ed. *The evolution and ecology of armadillos, sloths, and vermilinguas*. Washington, DC: Smithsonian Institution Press, 365-378.

Morford S, Meyers MA. 2003. Giant anteater (*Myrmecophaga tridactyla*) health care survey. *Edentata* 5: 5-20.

Murphy WJ, Eizirik E, Johnson WE, Zhang YP, Ryderk OA, O'Brien SJ. 2001. Molecular phylogenetics and the origins of placental mammals. *Nature* 409: 614-618.

Noss AJ, Cuéllar RL, Cuéllar E. 2008. Exploitation of Xenarthrans by the Guaraní-Isoseño indigenous people of the Bolivian Chaco: comparisons with hunting by other indigenous groups in Latin America, and implications for conservation. Em: Vizcaino SF, Loughry WJ, eds. *The biology of the Xenarthra*. Gainesville, FL: University Press of Florida, 244-254.

Patzl M, Schwarzenberger F, Osmann C, Bamberg E, Bartmann W. 1998. Monitoring ovarian cycle and pregnancy in the giant anteater (*Myrmecophaga tridactyla*) by faecal progestagen and oestrogen analysis. *Animal Reproduction Science* 53: 209-219.

Pereira Júnior HRJ, Jorge W, Costa MELT. 2004. Chromosome study of anteaters (Myrmecophagideae, Xenarthra): a preliminary report. *Genetics and Molecular Biology* 27: 391-394.

Ratter JA, Ribeiro JF, Bridgewater S. 1997. The Brazilian Cerrado vegetation and threats to its biodiversity. *Annals of Botany* 80: 223-230.

Ribeiro MC, Metzger JP, Martensen AC, Ponzoni FJ, Hirota MM. 2009. The Brazilian Atlantic Forest: how much is left, and how is the remaining forest distributed? Implications for conservation. *Biological Conservation* 142: 1141-1153.

Rossi LF, Chirino MG, Luaces JP, Merani MS. 2014. Determination of the karyotype of the giant anteater *Myrmecophaga tridactyla* (Myrmecophagidae: Xenarthra) using classical and molecular cytogenetic techniques. *Italian Journal of Zoology* 81: 322-327.

Sandoval-Gómez VE, Ramírez-Chaves HE, Marín D. 2012. Registros de hormigas y termitas presentes en la dieta de osos hormigueros (Mammalia: Myrmecophagidae) en tres localidades de Colombia. *Edentata* 13: 1-9.

Shaw JH, Machado-Neto J, Carter TS. 1987. Behavior of free-living giant anteaters (*Myrmecophaga tridactyla*). *Biotropica* 19: 255-259.

Silveira L, Rodrigues FHG, Jácomo ATA, Diniz Filho JAF. 1999. Impacts of wildfires on the megafauna of the Emas National Park, central Brazil. *Oryx* 33: 108-114.

Superina M, Miranda F, Plese T. 2008. Maintenance of Xenarthra in captivity. Em: Vizcaino SF, Loughry WJ, eds. *The biology of the Xenarthra*. Gainesville, FL: University Press of Florida, 232-243.

Wetzel RM. 1982. Systematics, distribution, ecology, and conservation of South American edentates. Em: Mares MA, Genoways HH, eds. *Pymatuning Symposia in Ecology, volume 6: mammalian biology in South America*. Linesville, PA: University of Pittsburgh, 345-375.

CAPÍTULO I

Research article

Population genetic structure, dynamics and historical demography of the giant anteater *Myrmecophaga tridactyla* Linnaeus, 1758 (Pilosa: Myrmecophagidae)

Raphael Teodoro Franciscani Coimbra, Rafael Félix de Magalhães, Flávia Regina Miranda and Fabrício Rodrigues dos Santos*

Laboratório de Biodiversidade e Evolução Molecular, Departamento de Biologia Geral, Instituto de Ciências Biológicas, Universidade Federal de Minas Gerais, Belo Horizonte, MG, Brazil

Running title: Phylogeography of *Myrmecophaga tridactyla*

***Correspondence:** Fabrício R. Santos. Laboratório de Biodiversidade e Evolução Molecular, Departamento de Biologia Geral, Instituto de Ciências Biológicas, Universidade Federal de Minas Gerais, Av. Antônio Carlos 6627, PO Box 486, 31270-010 Belo Horizonte, Minas Gerais, Brazil. E-mail: fsantos@icb.ufmg.br.

Abstract

Myrmecophaga tridactyla is a strictly myrmecophagous xenarthran species that ranges from Honduras to northern Argentina occupying various habitats, from grassland and floodplains to forests. It is constantly threatened by poaching, habitat loss and fragmentation, wildfires and road kills; thus, holding a vulnerable conservation status. Here, we investigate the population structure, dynamics and historical demography of Brazilian populations of *M. tridactyla*. We analyzed 2854 bp of mitochondrial and nuclear sequences of 106 individuals from Cerrado, Pantanal, and both Amazon and Atlantic Forests. The study was approached through haplotype networks construction, Bayesian clustering analysis, AMOVA, estimates of haplotype and nucleotide diversities, rarefied/extrapolated haplotype richness curves, migration model selection and multilocus demographic reconstruction. The mitochondrial DNA indicated two moderately distinct genetic clusters (φ_{ST} = 0.3275): one in the Amazon biome, [AM]; and another in the Cerrado, Pantanal and Atlantic Forest biomes, [CEPTAF]. The species' mitochondrial haplotype diversity (h = 0.7623) was moderate when compared to other threatened and non-threatened species. At the population level, [CEPTAF] tends to have a higher mitochondrial haplotype richness than [AM], likely due to a smaller effective population size for the latter. A gene flow pattern from [AM] to [CEPTAF] was detected with P = 0.8476, possibly due to both greater food availability and habitat heterogeneity in both Cerrado and Pantanal. Moreover, we recovered a ~ 7.5-fold population expansion since 60 kya and discussed hypotheses for its causes. In conclusion, we demonstrated the influence of ecological characteristics of *M. tridactyla* on both the natural history and genetic diversity configuration of its populations, reinforcing the importance of the Cerrado for the species' conservation.

Keywords: Amazon - Cerrado - conservation genetics - gene flow - model selection - phylogeography - population expansion - skyline plot - spatial genetics - Xenarthra

1. Introduction

The giant anteater (*Myrmecophaga tridactyla* Linnaeus, 1758) is a xenarthran species highly specialized for myrmecophagy. Many of its morphological adaptations reflect this feeding habit, such as complete absence of teeth and presence of an elongated protractile tongue (Naples, 1999; Casali et al., 2017). It is also the largest of all four anteater species, with adults averaging 2 m and 33 kg (Gardner, 2007). *M. tridactyla* currently ranges from Honduras southwards to northern Argentina (Miranda, Bertassoni & Abba, 2014) and new records of the species were recently reported in the Magdalena-Urabá moist forest ecoregion in Colombia (Figel et al., 2015). Giant anteaters are flexible regarding environmental occurrence, inhabiting from grasslands and floodplains to forests (Wetzel, 1982; Medri, Mourão & Rodrigues, 2011). Nevertheless, they seem to benefit from heterogeneous landscapes (Quiroga et al., 2016; Bertassoni et al., 2017; Di Blanco et al., 2017). Foraging commonly takes place in grasslands or shrub savannas, whereas covered habitats like forest patches and shrubs are used for resting, temperature buffering and protecting against predators (Shaw, Machado-Neto & Carter, 1987; Camilo-Alves & Mourão 2006; Mourão & Medri, 2007; Desbiez & Medri, 2010; Di Blanco, Pérez & Di Bitetti, 2015; Bertassoni et al., 2017). Despite that, habitat selection may be influenced by both local climate and availability of the habitat type (Di Blanco et al., 2017). Concentration of food resources accessible at the ground level, higher in dry open biomes like the Chaco and the Cerrado compared to moist forests, may also support a higher abundance of the species in those regions (Quiroga et al., 2016).

Concerning its conservation, *M. tridactyla* apparently tolerates a certain level of human impact, such as cattle ranching and moderate fires (Shaw et al., 1987; Quiroga et al., 2016). Likewise, Zimbres et al. (2013) did not observe actual effects of habitat fragmentation on the abundance and probability of occupancy of giant anteaters in the Cerrado of central Brazil. Regardless of that, the species already likely disappeared from Belize, El Salvador, Guatemala, Uruguay and the Brazilian states of Espírito Santo, Rio de Janeiro, Rio Grande do Sul and Santa Catarina (Miranda et al., 2014). Poaching (Leeuwenberg, 1997; Noss, Cuéllar & Cuéllar, 2008; Meritt, 2008), habitat loss and fragmentation (Harris et al., 2005; Klink & Machado, 2005; Ribeiro et al., 2009), wildfires (Silveira et al., 1999) and road kills (Cáceres et al., 2010; Cunha, Moreira & Silva, 2010; Freitas, Justino & Setz, 2014) pose a constant threat to *M. tridactyla* over much of its range and are thought to be the main causes of its recent population decline (Miranda et al., 2014). Furthermore, there are evidences for a species' trend to avoid heavily disturbed areas in which the presence of humans, cattle and dogs is high, and also for the importance of conserved forest vegetation in the species' non-preferred areas (Shaw et al., 1987; Vynne et al., 2011; Di Blanco et al., 2015). For these reasons, the giant

anteater is listed as vulnerable on the IUCN Red List of Threatened Species (Miranda et al., 2014) and appears in CITES Appendix II (http://www.cites.org).

Genetic variability is an important feature for the continued maintenance of wild populations; however, threatened species are more susceptible to losses in that parameter due to, among other factors, their generally small and/or declining effective population sizes (Frankham, 2005). Acknowledging that and the limited repertoire of population genetic studies regarding the giant anteater (Garcia et al., 2005; Collevatti et al., 2007), Clozato et al. (2017) assessed the population structure and genetic diversity of the species in Brazil using mitochondrial (mtDNA) and nuclear (nDNA) markers. That work collected samples from both Amazon (AM) and Atlantic Forests (AF), Pantanal wetlands (PT), and Cerrado (CE). Their findings showed an overall high genetic diversity for the species and signs of population expansion. Moreover, the authors detected a notable genetic structure between populations from the CE/PT and AM and a possible past connection between both AM and AF. Nevertheless, there is no data on the timing and magnitude of the population expansion. Furthermore, assessing the gene flow pattern between populations is also essential for phylogeography and conservation management, since it can affect their ecological and evolutionary properties (Whitlock & McCauley, 1999), but this was not addressed in the previous work.

Herein, we investigated the (i) geographic patterns of genetic diversity, (ii) gene flow dynamics and (iii) historical population size changes of *M. tridactyla* in the Brazilian territory through phylogeographic and spatial genetics analyses. Our results provided valuable information on both the evolutionary history and conservation of the giant anteater, a vulnerable and otherwise poorly known species.

2. Materials and methods

2.1. Biological samples and DNA extraction

We used DNA samples from 77 individuals of *M. tridactyla* from Clozato et al. (2017) and added 28 new tissue samples, mainly from muscle, blood, skin or hair from road-killed animals and museum specimens, but also a few from wild and captive individuals of known origin. Overall, we sampled 105 individuals from the Brazilian states of Amapá (n = 2), Goiás (n = 29), Minas Gerais (n = 25), Mato Grosso (n = 12), Mato Grosso do Sul (n = 17), Pará (n = 4), Paraná (n = 8), Roraima (n = 1) and São Paulo (n = 7). Thus, we covered the Brazilian biomes of Cerrado (CE, n = 78), Pantanal (PT, n = 11), Amazonia (AM, n = 8), and Atlantic Forest (AF, n = 8). We also retrieved mtDNA sequences of a French Guiana specimen from

GenBank (accession number KT818549) for computational analyses. Figure 1 and Table S1 present a map of sampling localities and a detailed list of samples, respectively.

Tissue samples were preserved in 70% ethanol and the DNA was extracted through standard phenol-chloroform protocol (Sambrook & Russell, 2001). Concentration of extracted DNA was assessed in a NanoDrop 2000 Spectrophotometer, and work dilutions were stored at -20°C. The remaining DNA were deposited at Laboratório de Biodiversidade e Evolução Molecular (LBEM) at the Universidade Federal de Minas Gerais (UFMG), in Brazil (Table S1).

2.2. PCR amplification and sequencing

Partial sequences of the mitochondrial $tRNA^{Thr}$/$tRNA^{Pro}$/hypervariable I contiguous regions (HVI for simplicity) and Cytochrome b (Cytb) gene, and an nDNA fragment of the Recombination-Activating Gene 2 (RAG2) published in Clozato et al. (2017) for 77 and 47 individuals, respectively, were included in this work. PCR amplifications were carried out for the remaining samples for HVI, Cytb and RAG2. Additionally, other two commonly used partial nDNA markers were amplified for all the 105 samples: the exon 28 of the von Willebrand Factor (vWF) gene and the Brain-Derived Neurotrophic Factor (BDNF) gene. The primers used here are presented in Table 1. PCR conditions varied between samples as follows: a final volume of 15 or 25 µL containing 20-100 ng of template DNA, 1 x reaction buffer, 1.5 or 3.0 mM $MgCl_2$, 100 µM dNTPs, 0.2 µM of each primer, 0.5 mg/mL of BSA adjuvant and 0.2 or 0.3 U of Platinum® *Taq* DNA Polymerase. Thermocycler programs started with 3 min at 95°C; followed by 35 cycles of 30 s at 95°C for denaturation, 45 s at 52°C (HVI and Cytb), 57°C (RAG2 and vWF) or 49°C (BDNF) for annealing; 1 min at 72°C for extension; and 5 min at 72°C. Adjustments in the primers annealing temperatures were necessary in some cases. PCR products were visualized in 1% agarose gel, purified through polyethylene glycol 20% precipitation (Santos Júnior, Santos & Silveira, 2015, modified from Sambrook & Russell, 2001) and sequenced in an ABI 3130xl Genetic Analyzer.

2.3. Sequence editing and haplotype phasing

Electropherograms were interpreted, assembled and pre-aligned in SeqScape v.2.6 (Applied Biosystems). Alignments were constructed with Clustal W (Thompson, Higgins & Gibson, 1994) implemented in MEGA7 (Kumar, Stecher & Tamura, 2016). Haplotype phase inference for each nDNA marker in heterozygous individuals was accomplished with SeqPHASE (Flot, 2010) and PHASE v.2.1.1 (Stephens, Smith & Donnelly, 2001; Stephens &

Scheet, 2005). To check for consistency, we performed three independent runs for 1000 iterations for each marker with a phase threshold of 0.9.

2.4. Assessing spatial genetic patterns

The relationships between haplotypes were visualized in median-joining phylogeographic networks (Bandelt, Forster & Röhl, 1999) for concatenated mtDNA sequences and for each nDNA *locus* with PopART v.1.7 (Leigh & Bryant, 2015).

Inferences on the K number of genetic clusters and detection of genetic discontinuities on the landscape were performed with the R v.3.4.0-patched (R Core Team, 2017) package Geneland v.4.0.6 (Guillot, Mortier & Estoup, 2005; Guillot, Estoup, et al., 2005; Guillot, 2008; Guillot, Santos & Estoup, 2008) using concatenated mtDNA. This method implements Markov Chain Monte Carlo (MCMC) algorithm and free colored Voronoi tessellation to cluster individuals, without any *a priori* knowledge on population units and limits, by minimizing both Hardy-Weinberg and linkage disequilibrium and incorporating geographic information in the analyses (Guillot, Estoup, et al., 2005). Since our interest focused on finding the more pronounced population genetic structure, we chose the spatially explicit uncorrelated allele frequencies model. We ran 20 independent MCMC for 10,000,000 iterations, thinning each 1,000, from which we chose the one with the highest value of average log posterior probability. Uncertainty on coordinates was set to 0.36 (~ 40 km) to accommodate the largest estimates of the species' home range (Montgomery & Lubin, 1977; Di Blanco et al., 2017) and the rough approximations of some geographic coordinates. K was left to vary from 1 to 10, the maximum rate of Poisson process was set equal to the number of individuals and the maximum number of *nuclei* was set to the triple of that, as recommended by Guillot, Estoup, et al. (2005). Following that, we measured the concatenated mtDNA diversity within and among the resultant clusters through an analysis of molecular variance (AMOVA; Excoffier, Smouse & Quattro, 1992) and estimated the haplotype (h) and nucleotide (π) diversities on Arlequin v.3.5 (Excoffier & Lischer, 2010). The distance method selected for calculations was the Kimura-2P (Kimura, 1980). Furthermore, we performed an interindividual Mantel test with $\log_{10}$-transformed geographic and genetic distances for 1000 permutations on AIS (Miller, 2005) to test for isolation by distance.

2.5. Estimating rarefied/extrapolated haplotype richness curves

Community ecologists and conservation biologists commonly use rarefaction and extrapolation techniques to estimate and compare species richness across multiple

assemblages that may vary in size (Gotelli & Colwell, 2011; Colwell et al., 2012). Here, we apply the same principle to compensate the bias introduced by discrepant sample sizes between populations in the results of genetic diversity analyses. We used the R package iNEXT v.2.0.12 (Chao et al., 2014; Hsieh, Ma & Chao, 2016) to compute and plot integrated rarefaction and extrapolation (R/E) accumulation curves for species richness, where the 'species' were substituted for 'haplotypes'. Three types of curves – (1) a sample size-based, (2) a coverage-based and (3) a sample completeness curve – were constructed for a reference sample size equal to the number of individuals of the largest genetic cluster defined by Geneland. We chose the largest instead of the smallest population size as a reference to visualize possible trends in estimates of genetic diversity for the smaller populations with increasing sample sizes. The 95% confidence interval (CI) for each asymptote was assessed through 1,000 bootstrap replicates.

2.6. Comparing migration scenarios

We used an approach based on Carstens et al. (2013) and Magalhães et al. (2017) to test between scenarios of split genealogical lineages versus a single cohesive lineage. Historical patterns of mtDNA gene flow for different migration models were estimated under a coalescent framework using the Bayesian implementation of Migrate-n v.3.6.11 (Beerli, 2006). Our models consisted of (1) a null hypothesis of a single panmictic population, (2) all possible migration scenarios between populations identified by Geneland and (3) a model where these populations were isolated (Figure 2). We set an empirical transition/transversion ratio (R_{mtDNA} = 2.44) calculated with the GTR substitution model (Tavaré, 1986) on MEGA7 and estimated the migration parameters in terms of mutation-scaled effective immigration rate M (m/μ) and mutation-scaled effective population sizes Θ ($N_e\mu$). Initial runs with a full migration matrix model allowed to set adequate parameter bounds. For the final runs, we assumed a uniform prior for Θ (minimum = 0, maximum = 0.015, delta = 0.0015) and an exponential prior for M (minimum = 0, mean = 1500, maximum = 3500). All other parameters were left with default options. Three parallel replicates were run for each model using a static heating scheme with 20 heated chains in which "temperatures" increased according to the program's suggested range of values. For each run, we discarded 15,000 steps and recorded 150,000 with a sampling increment of 1,000. Convergence was checked by unimodality of parameters' posterior distributions and by assessing both effective sample sizes (ESS) and acceptance ratio values. Model selection was performed through the comparison of the marginal likelihood of each model – calculated through the thermodynamic integration estimator with cubic Bézier-spline approximation – by

means of Bayes factors (Beerli & Palczewski, 2010). Analyses were run on CIPRES Science Gateway v.3.3 (Miller, Pfeiffer & Schwartz, 2010) computer cluster.

2.7. Inferring the historical demography of the giant anteater

To include a time scale in our demographic inference, we first conducted a molecular dating analysis to estimate a reference clock rate for the partial Cytb sequence. Hence, in this first step, we included only the unique *M. tridactyla* Cytb haplotypes and the two *Tamandua* species (KT818551 and KT818552) as outgroups. The molecular dating was performed in BEAST v.2.4.5 (Bouckaert et al., 2014) using the transition/transversion split option of the bModelTest package (Bouckaert & Drummond, 2017), a strict clock with a birth-death tree prior and a lognormal prior on calibration (mean in real space, offset = 7.0, mean = 6.35 and standard deviation = 0.398). Hard minimum and soft maximum age constraints for the Myrmecophagidae node were based on the 95% credibility interval (19.8-7.0 mya) from Gibb et al. (2016). We run three independent MCMC for 50,000,000 generations sampling each 5,000 and checked trace files on Tracer v.1.6 (Rambaut et al., 2014) to ensure chain convergence and good ESS values. LogCombiner was used to combine trace files from all runs with a 50% burn-in and the mean value of the 'clockRate' parameter was recovered with Tracer.

Subsequently, we carried out a historical demography reconstruction on *M. tridactyla* through the extended Bayesian skyline plot method (EBSP; Heled & Drummond, 2008) using our complete dataset with mtDNA and nDNA. The EBSP was also performed in BEAST 2 with unlinked site and clock models, and trees linked only for mtDNA. Once more, the transition/transversion split option of bModelTest was used in combination with strict clocks for all markers. In addition, to convert the x-axis of the EBSP result in time units, the clock rate of the Cytb was fixed to the value estimated in the previous molecular dating analysis, whereas all other clock rates were estimated relative to that. The weights of the operators affecting the population function were increased by a factor of four to even the frequency of proposals regarding the population function with those that change the trees during the MCMC (see EBSP tutorial available from https://www.beast2.org/tutorials/). The CIPRES Science Gateway was used to run three independent MCMC for 1,000,000,000 generations sampling each 100,000. At the end of the analyses, we checked both convergence and high values of ESS on Tracer. EBSPs were plotted on R with a 10% burn-in using the script provided with the EBSP tutorial.

3. Results

3.1. Sequencing and haplotype phasing

We obtained mtDNA sequences of HVI (450 bp) and Cytb (534 bp) for all new samples. On the other hand, nDNA *loci* exhibited lower amplification efficiency. RAG2 sequences for 21 specimens were generated, however, only 12 spanned the maximum length of the external primers (745 bp), the other nine only amplified and sequenced with nested primers (481 bp). In turn, vWF (546 bp) and BDNF (579 bp) were sequenced for 60 and 65 individuals, respectively. AM specimens could not be sequenced for any of the nDNA *loci*.

Haplotype phasing of nDNA *loci* showed consistent results and we only report here the cases in which our initial standards were not matched. For RAG2, genotypes of four individuals (LabBMC0122, M0696, M1678 and SCMT04) could not be resolved with the 0.9 phase threshold; therefore, we kept the allele combinations with the highest probability. For BDNF, the genotype of one individual (TBC013) could not be determined by any means due to two allele combinations with equal probabilities. In this case, we retained the ambiguous base symbol.

Shorter RAG2 sequences and the ambiguous BDNF sequences could not be included in the haplotype networks.

3.2. Spatial patterns and genetic diversity characterization

The mtDNA network exhibited 33 closely related haplotypes (Figure 3A), most differing by a single mutation, with a total $h = 0.7623$ and a $\pi = 0.0021$ (Table 2). We observed a largely predominant haplotype mainly occurring in the CE biome, and some level of haplotype sharing between CE and PT; CE, PT and AF; CE, AF and AM; and AF and AM. Moreover, AM haplotypes are clustered together in the network, except for the one from French Guiana that was retrieved from GenBank, suggesting some degree of genetic structure. On the other hand, nDNA networks, which lacked AM representatives, did not show geographic correlation and evidenced haplotype sharing among the included biomes (Figure 3B-D). RAG2, vWF and BDNF presented 9, 10 and 5 haplotypes, respectively. Due to the high amount of missing data and the absence of AM samples between nDNA sequences, we focused the remaining spatial analyses on mtDNA data alone.

Geneland results (Figure 4) were in agreement with the mtDNA network patterns and consistently indicated $K = 2$ as the most likely value for that variable, clustering all individuals from AM in one group, from now on called [AM], and the remaining individuals from CE, PT and AF in another one, named [CEPTAF]. Consequently, we have genetic clusters with largely

discrepant sample sizes: 9 for [AM] and 97 for [CEPTAF]. Values of posterior probability for cluster membership were > 0.7 for [CEPTAF] and mostly > 0.9 for [AM], with only one individual (M0705), geographically intermediate between the two clusters, showing P = 0.56 for the latter group. The AMOVA showed a φ_{ST} = 0.3275 and we follow Meirmans (2015) in not reporting its P-value, since it would be meaningless due to non-independence of data. Furthermore, [CEPTAF] presented h = 0.7204 and π = 0.0019, whereas [AM] had h = 0.8889 and π = 0.0027 (Table 2). Finally, the Mantel test revealed a slight positive correlation between genetic and geographic distances, with r = 0.1213 (P = 0.0040; Figure 5).

3.3. Integrated rarefaction/extrapolation curves

The sample size-based R/E curve (Figure 6A) showed that, when estimated sample sizes are smaller than 20 individuals, the haplotype richness is expected to be higher for [AM]. However, after that point, the curve for [AM] starts to plateau, while it continues to grow for [CEPTAF]. Hence, we expect that, for larger sample sizes, the haplotype richness will be higher for [CEPTAF]. Nonetheless, the extrapolated asymptote for [AM] presented a large 95% CI, illustrating the difficulties imposed by its small sample size.

The sample completeness R/E curve (Figure 6B) indicated that our estimated current sample coverage for [AM] haplotypes was ~ 58%, whereas for [CEPTAF] it was ~ 83%. Although the 95% CI is also large, the expected number of samples needed for [AM] to achieve the same level of coverage of [CEPTAF] would be around 25, which contrasts with our current sampling.

The coverage-based R/E curve (Figure 6C), which integrates the two previous curves, evidenced that increasing sample coverage beyond 50% greatly increased haplotype richness for [CEPTAF]. Despite that, a continued increase in sample coverage for [AM] would result in a much less pronounced gain in that index. Moreover, considering the 95% CI, significant differences in haplotype richness between the two clusters are expected to arise after passing 65% of sample coverage, with [CEPTAF] showcasing higher values than [AM].

3.4. Evidence for unidirectional gene flow

In our Migrate-n analyses, parameter estimates generally overlapped (Table S2), with the exception of the $\Theta_{[AM]}$ for the isolated populations model, which explored values much closer to zero, possibly due to an uninformative amount of data imposed by the small sample size of that population. In the scenarios that considered migration, gene flow was higher from

[AM] to [CEPTAF]. In addition, $M_{[AM]\rightarrow[CEPTAF]}$ presented bell-shaped posterior distributions that did not include zero in their credibility intervals, while $M_{[CEPTAF]\rightarrow[AM]}$ showed more skewed distributions that included zero, when migration was bidirectional, or were much wider, when it was unidirectional. Assuming an equal *a priori* probability of 20% for each of the five models tested in Migrate-n and considering that probability as a threshold for rejecting competing hypotheses through Bayes factors comparison, we could clearly discard four scenarios (Table 3). The best-fit migration model selected (P = 0.8476) was the one that considered two separate populations with gene flow from [AM] to [CEPTAF]. For this model, we had mode values of $\Theta_{[AM]}$ = 0.00086, $\Theta_{[CEPTAF]}$ = 0.00345 and $M_{[AM]\rightarrow[CEPTAF]}$ = 1368.5, which translate into an effective number of migrants per generation (N_m) of 1.177 from [AM] to [CEPTAF], through the equation $N_m = \Theta M$.

3.5. Historical population expansion

Both the mtDNA and RAG2 phylogeographic networks (Figure 3A and D) displayed a star-shape pattern, with one most common haplotype originating various low frequency and closely related ones, suggesting recent population expansion. Furthermore, the molecular dating of the unique Cytb haplotypes resulted in a clock rate of 7.4513 x 10^{-3} substitutions/site/million years, which was used to produce a time-scaled EBSP for the whole species (Figure 7). The plot revealed a population growth that starts slowly at ca. 60 kya and largely increases since ca. 40 kya, reaching a present population size (N_eT) around 7.5 times the size of the original population when considering the graph's median. We recognize that population structure can affect the output of population size change inferences (Chikhi et al., 2010; Heller, Chikhi & Siegismund, 2013), nonetheless, in our case, this seems not to be a problem, since removing the samples from the smaller population (AM) did not alter the results (data not shown).

4. Discussion

We assessed the geographic patterns of genetic diversity, gene flow dynamics and ancestral demography of the giant anteater, shedding some light on the species' natural history and the current status of its populations. The clustering analysis indicated two main genetically distinct clusters in *M. tridactyla*: one correspondent to individuals from the AM biome, [AM]; and another equivalent to individuals from CE, PT and AF biomes, [CEPTAF]. Such spatial configuration could be misleading if it were a consequence of the large sampling gap between the north of AM and CE/PT. In that case, we would have captured, for instance, two extremes

of a cline of allele frequencies in a scenario of isolation by distance. However, besides the weak correlation between geographic and genetic distances demonstrated in the Mantel test, the mtDNA phylogeographic network also displayed a clustering of AM haplotypes, supporting the [AM] and [CEPTAF] spatial structure. Additionally, the scenario of a single panmictic population was discarded as one of the less likely models during the migration model selection. Taken together, these mtDNA results reinforce the presence of population structure in *M. tridactyla* and seem rather to reflect environmental differences between the occurrence areas of its genetic clusters: [AM] in a forested biome and [CEPTAF] in mostly open vegetation biomes. Thus, a kind of 'isolation by environment' (Wang & Bradburd, 2014) may better describe this pattern.

The observed φ_{ST} for such population structure was slightly smaller than the obtained by Clozato et al. (2017), but still a moderate value when compared to other phylogenetically or ecologically related species. For instance, *M. tridactyla* showed a φ_{ST} value higher than those reported for Paraguayan populations of the nine-banded armadillo (*Dasypus novemcinctus* Linnaeus, 1758; Frutos & Van Den Bussche, 2002) and the screaming hairy armadillo (*Chaetophractus vellerosus* (Gray, 1865); Nardelli et al., 2016). In turn, that value was much lower than those presented by Mexican populations of *D. novemcinctus* (Arteaga et al., 2012) and arboreal xenarthran species like the silky anteater (*Cyclopes didactylus* (Linnaeus, 1758); Coimbra et al., 2017) and the maned sloth (*Bradypus torquatus* Illiger, 1811; Lara-Ruiz, Chiarello & Santos, 2008; Schetino, Coimbra & Santos, 2017). Moreover, similar φ_{ST} estimates were found for incompletely isolated phylogeographic partitions of the jaguar (*Panthera onca* (Linnaeus, 1758); Eiziriki et al., 2001). This finding is not surprising, since we expect *M. tridactyla* to have great dispersal abilities because its home range can be quite large (up to 32.50 ± 7.64 km^2; Di Blanco et al., 2017; see also Montgomery & Lubin, 1977; Shaw et al., 1987; Miranda, 2004; Medri & Mourão, 2005; Macedo, 2008; Braga, 2010; Macedo, Azevedo & Pinto, 2010; Rojano et al., 2015; Bertassoni et al., 2017). Furthermore, the giant anteater's overall h and π for the mtDNA were lower than the observed for non-threatened species such as the nine-banded armadillo (Huchon et al., 1999; Frutos & Van Den Bussche, 2002; Arteaga et al., 2012) and the jaguar (Eiziriki et al., 2001). Nevertheless, the obtained h was higher than that found for the similarly vulnerable maned sloth, whereas π was slightly lower (Lara-Ruiz et al., 2008; Schetino et al., 2017). In this case, the widespread distribution and the ecological versatility of *M. tridactyla* may still be enough to secure moderate levels of h even in front of the decreasing population numbers, a fact that does not hold true for the maned sloth, which has a fragmented and restricted range in the AF (Lara-Ruiz et al., 2008; Schetino et al., 2017).

When comparing the two genetic clusters of *M. tridactyla*, [AM] showed h and π values higher than the estimated for [CEPTAF] and for the overall species. This result is likely

overestimated, since the R/E curves of haplotype richness for [AM] suggest that, although our sampling for this cluster was small, increasing the sample coverage would result in only limited gain in richness. On the other hand, [CEPTAF], which exhibited h and π values close to the total obtained for the species, can be even more diverse according to its R/E curves that still showed signs of haplotype richness increase with larger sample coverage. One possible explanation for this observation would be that [AM] may have a population size much smaller than [CEPTAF], and indeed, this might be the case. Quiroga et al. (2016) analyzed data from 40 camera trap studies conducted in 42 sites scattered across different biomes in the species continental range. They found that *M. tridactyla* is more frequently recorded in dry forests and grassland-savannas, although this latter was not confirmed, than in moist forests. Data on population densities in locations within the area of each identified genetic cluster would also be important to give us a more accurate indication of differences in population sizes. In fact, the giant anteater is expected to achieve its highest densities in the CE (Redford, 1994). Unfortunately, population densities for *M. tridactyla* are only available for a small number of sites, all of which have predominantly savanna-like vegetation containing a few forest fragments, which hinders fair comparisons (Eisenberg, O'Connell & August, 1979; Shaw, Carter & Machado-Neto, 1985; Shaw et al., 1987; Coutinho et al., 1997; Silveira et al., 1999; Miranda et al., 2006; Desbiez & Medri, 2010; Kreutz, Fischer & Linsenmair, 2012; Rojano, Miranda & Ávila, 2015). Nonetheless, one have to bear in mind that extrapolations of richness measures can only be made reliably up to double the size of a population due to increasing bias towards underestimation with larger sample sizes (Chao et al., 2014; Hsieh et al., 2016). Therefore, the early plateauing of the [AM] haplotype richness asymptote may be an artifact of the method, which is reflected in its large 95% CI.

Clozato et al. (2017) suggested a past connection between giant anteater populations from AM and AF due to haplotype sharing. Accordingly, we also observed a certain level of haplotype sharing between CE, AM and AF in the mtDNA network. Furthermore, our migration model selection indicated a small gene flow from [AM] to [CEPTAF]. However, the Migrate-n results may also reflect the species ecological characteristics, considering *M. tridactyla*'s preference for heterogeneous landscapes (Quiroga et al., 2016; Bertassoni et al., 2017; Di Blanco et al., 2017) and the discrepancies in food availability and/or accessibility between savanna-like environments and moist forests (Quiroga et al., 2016). In that sense, migrants from [AM] are much more likely to find suitable conditions in the area occupied by [CEPTAF] than the inverse scenario. That is due to primarily open biomes, such as PT (Silva et al., 2000) and CE (Cardoso da Silva & Bates, 2002), generally offering both greater habitat heterogeneity and abundance of ants and termites. Therefore, historically, individuals from [AM] that eventually enter either CE or PT, which are in immediate contact with AM, might end up

establishing there and contributing to the next generation. Migrants from [CEPTAF], however, may avoid crossing to AM or at least they do not infiltrate further into the biome; thus, even if some of them reproduce there, it would be in much lower proportions. Hence, the apparent isolation by environment pattern observed for the population structure could be due to this biased dispersal and gene flow (Wang & Bradburd, 2014), which are influenced by the giant anteater's ecology. It is important to note, however, that Migrate-n assumes that "population sizes are constant through time or are randomly fluctuating around an average population size" (Beerli, 2009). Our dataset violates this assumption. With growing populations, as the EBSP showed to be the case for *M. tridactyla*, Migrate-n tends to underestimate the effective population size (Beerli, 2009). This, together with the hugely different sample sizes of [AM] and [CEPTAF], may have exerted some influence in the results and, thus, we recommend interpreting them with caution.

Current giant anteater numbers are thought to be currently declining due to poaching (Leeuwenberg, 1997; Noss et al., 2008; Meritt, 2008), habitat loss and fragmentation (Harris et al., 2005; Klink & Machado, 2005; Ribeiro et al., 2009), wildfires (Silveira et al., 1999) and road kills (Cáceres et al., 2010; Cunha et al., 2010; Freitas et al., 2014). Historically, however, *M. tridactyla* seems to have experienced a large population expansion (~ 7.5-fold) since 60-40 kya. Additionally, both the mtDNA and RAG2 networks show signs of recent expansion, with various rare haplotypes derived from a much more frequent one mostly characteristic of the CE biome. This is in line with the findings of Clozato et al. (2017), which suggested a scenario of recent population expansion for the giant anteater based on a star-shaped mtDNA network, a negative Tajima's D value (-2.02 with $P < 0.0001$) and a unimodal mismatch distribution plot. It is important to note, though, that our sampling unintentionally favored the CE when compared to the other biomes. Nevertheless, these results led us to think about a possible correlation between the giant anteater's population increase and the supposed expansion of open vegetation biomes during the last glacial period (ca. 110-12 kya; Haffer, 1969). Recent modeling studies, however, indicate that the CE achieved its maximum extent during the last interglacial period (ca. 130-115 kya), which was then followed by a retraction during the last glacial period, possibly related to both decreased precipitation and temperature (Werneck et al., 2012; Bueno et al., 2016). A second hypothesis would be an increase in food availability during the last glacial period. Unfortunately, to our knowledge, there are no works evaluating possible changes in ant and termite communities caused by Quaternary climatic oscillations. Finally, late Pleistocene megafaunal extinction, globally occurring from ca. 50-7 kya (Barnosky, 2008), may have been linked to the population expansion in *M. tridactyla* through the extirpation of contemporary predators and competitors. However, although the timing of extinction is still poorly established in South America, growing evidence suggest that its pace

only accelerated between 13.5 and 11.2 kya, with some taxa lasting until ca. 8 kya (Barnosky & Lindsey, 2010; Prado, Martinez-Maza & Alberdi, 2015; Villavicencio et al., 2016). These estimates largely post-dates our obtained timing for the giant anteater's population expansion. Thus, the trigger for the population expansion of *M. tridactyla* is still unclear and needs further investigations.

From a conservation standpoint, Zimbres et al. (2012) demonstrated that Brazilian reserves for integral protection (IPs) cover less than 10% of the giant anteater's suitable areas modeled for the present and for the future under climate change. Despite that, if reserves for sustainable use (SUs) and indigenous reserves are also considered, the species is adequately protected (Zimbres et al., 2012). Nevertheless, these SUs are mostly located in AM, as shown by Zimbres et al. (2012). The [AM] cluster identified here is also located in AM, and this population is more likely to suffer from loss of genetic diversity by stochastic processes due to its apparent small population size (Frankham, 2005). However, even with the existing protected areas (PAs) in AM, our limited sampling and the lack of information about the species in that region prevent us to assume an adequate maintenance of the genetic diversity for [AM]. For that reason, we emphasize the need for more studies on the giant anteater in AM. On the other hand, besides the apparent larger population size for [CEPTAF], the number of PAs within its occurrence area is much smaller (Zimbres et al., 2012). Françoso et al. (2015) showed that PAs represent only 6.5% of the native CE remnants and that SUs use are ineffective in protecting its biodiversity. In addition, Diniz & Brito (2015) demonstrated that, of the 18 federal PAs in the CE in which the giant anteater occurs, only 11 are capable of maintaining viable populations for the next 100 years under an optimistic scenario of population density, whereas only three accomplish that in a pessimistic one. Beyond that, both CE and AF have been massively devastated with only about 45% (Klink & Machado, 2005) and 11.7% (Ribeiro et al., 2009) of their original vegetation remaining, respectively. Zimbres et al. (2012) already stressed the ecological importance of CE for the conservation of xenarthran species, particularly *M. tridactyl*a, and suggested both PT and northern CE as priority areas for future conservation. As such, our findings also highlight the urgency for increasing of the number and the extent of IPs in those regions, so that the maintenance of the genetic diversity of [CEPTAF] can be granted.

Obtaining a representative sampling of a widespread animal species is an arduous task, even more so when such species presents low population densities in most of its range. We cannot discard the possibility that our AF samples are actually from wandering CE individuals. Those samples were treated here as from AF because they were collected from individuals in areas within the original distribution of that biome. However, sampling localities were in proximity with the CE in the Paraná state. Besides that, native forested areas in the AF

were drastically transformed by human activity and its remnants are largely fragmented (Ribeiro et al., 2009). Furthermore, the large difference in sample sizes imposed by the sparse sampling of AM individuals herein may have biased some of the analyses. Recognizing that, we adapted R/E techniques from community ecology studies to minimize the impact on genetic diversity analyses and included a null model of panmixia in the migration model selection to contrast the population structure found. These approaches are not a cure for the problem and, for that reason, our results should be interpreted carefully. Thus, we encourage both new studies and sampling efforts, mainly in the AM and in regions outside Brazilian borders, which are much needed to visualize a more complete picture of the species' evolutionary history. However, notwithstanding its inherent limitations, this study presented evidences from different sources all converging to support the presence of environmental population structure, ecologically-driven gene flow and historical demographic expansion in *M. tridactyla*.

5. Acknowledgments

This study was funded by FAPEMIG, CNPq and Boticário Group Foundation. We are grateful to José Eustáquio, Arnaud Desbiez, Carmen Ruiz, Pedro Galetti, Ana Luiza Queiroz, Evanguedes Kalapothakis, Fernanda Braga and the Capão da Imbuia Museum of Natural History for providing some samples. We also thank Gustavo Kuhn and Ubirajara Oliveira for helpful comments on an earlier version of the manuscript. The authors declare no conflict of interests. R.T.F.C. received a CAPES M.Sc. scholarship; R.F.M. holds a CNPq post-Ph.D. fellowship; F.R.M. received a CAPES Ph.D. scholarship; and F.R.S. holds a CNPq research fellowship.

6. References

Arteaga MC, Piñero D, Eguiarte LE, Gasca J, Medellín RA. 2012. Genetic structure and diversity of the nine-banded armadillo in Mexico. *Journal of Mammalogy* 93: 547-559.

Bandelt H, Forster P, Röhl A. 1999. Median-joining networks for inferring intraspecific phylogenies. *Molecular Biology and Evolution* 16: 37-48.

Barnosky AD. 2008. Megafauna biomass tradeoff as a driver of Quaternary and future extinctions. *Proceedings of the National Academy of Sciences of the United States of America* 105: 11543-11548.

Barnosky AD, Lindsey EL. 2010. Timing of Quaternary megafaunal extinction in South America in relation to human arrival and climate change. *Quaternary International* 217: 10-29.

Beerli P. 2006. Comparison of Bayesian and maximum-likelihood inference of population genetic parameters. *Bioinformatics* 22: 341-345.

Beerli P. 2009. How to use Migrate or why are Markov chain Monte Carlo programs difficult to use? In: Bertorelle G, Bruford MW, Hauffe HC, Rizzoli A, Vernesi C, eds. *Population genetics for animal conservation*. New York, NY: Cambridge University Press, 42-79.

Beerli P, Palczewski M. 2010. Unified framework to evaluate panmixia and migration direction among multiple sampling locations. *Genetics* 185: 313-326.

Bertassoni A, Mourão G, Ribeiro RC, Cesário CS, Oliveira JP, Bianchi RC. 2017. Movement patterns and space use of the first giant anteater (*Myrmecophaga tridactyla*) monitored in São Paulo State, Brazil. *Studies on Neotropical Fauna and Environment* 52: 68-74.

Bouckaert RR, Drummond AJ. 2017. bModelTest: bayesian phylogenetic site model averaging and model comparison. *BMC Evolutionary Biology* 17(42).

Bouckaert R, Heled J, Kühnert D, Vaughan T, Wu C, Xie D, Suchard MA, Rambaut A, Drummond AJ. 2014. BEAST 2: a software platform for bayesian evolutionary analysis. *PLoS Computational Biology* 10: e1003537.

Braga FG. 2010. Ecologia e comportamento de tamanduá-bandeira *Myrmecophaga tridactyla* Linnaeus, 1758 no município de Jaguariaíva, Paraná. Unpublished D. Phil. Thesis, Universidade Federal do Paraná.

Bueno ML, Pennington RT, Dexter KG, Kamino LHY, Pontara V, Neves DM, Ratter JA, Oliveira-Filho AT. 2016. Effects of Quaternary climatic fluctuations on the distribution of Neotropical savanna tree species. *Ecography* 39: 1-12.

Cáceres NC, Hannibal W, Freitas DR, Silva EL, Roman C, Casella J. 2010. Mammal occurrence and roadkill in two adjacent ecoregions (Atlantic Forest and Cerrado) in south-western Brazil. *Zoologia* 27: 709-717.

Camilo-Alves CSP, Mourão GM. 2006. Responses of a specialized insectivorous mammal (*Myrmecophaga tridactyla*) to variation in ambient temperature. *Biotropica* 38: 52-56.

Cardoso da Silva JM, Bates JM. 2002. Biogeographic patterns and conservation in the South American Cerrado: a tropical savanna hotspot. *BioScience* 52: 225-234.

Carstens BC, Brennan RS, Chua V, Duffie CV, Harvey MG, Koch RA, Mcmahan CD, Nelson BJ, Newman CE, Satler JD, Seeholzer G, Posbic K, Tank DC, Sullivan J. 2013. Model

selection as a tool for phylogeographic inference: an example from the willow *Salix melanopsis*. *Molecular Ecology* 22: 4014-4028.

Casali DM, Martins-Santos E, Santos ALQ, Miranda FR, Mahecha GAB, Perini FA. 2017. Morphology of the tongue of Vermilingua (Xenarthra: Pilosa) and evolutionary considerations. *Journal of Morphology* ahead of print.

Chao A, Gotelli NJ, Hsieh TC, Sander EL, Ma KH, Colwell RK, Ellison AM. 2014. Rarefaction and extrapolation with Hill numbers: a framework for sampling and estimation in species diversity studies. *Ecological Monographs* 84: 45-67.

Chikhi L, Sousa C, Luisi P, Goossens B, Beaumont MA. 2010. The confounding effects of population structure, genetic diversity and the sampling scheme on the detection and quantification of population size changes. *Genetics* 186: 983-995.

Clozato CL, Miranda FR, Lara-Ruiz P, Collevatti RG, Santos FR. 2017. Population structure and genetic diversity of the giant anteater (*Myrmecophaga tridactyla*: Myrmecophagidae, Pilosa) in Brazil. *Genetics and Molecular Biology* 40: 50-60.

Coimbra RTF, Miranda FR, Clozato CL, Schetino MAA, Santos FR. 2017. Phylogeographic history of South American populations of the silky anteater *Cyclopes didactylus* (Pilosa: Cyclopedidae). *Genetics and Molecular Biology* 40: 40-49.

Collevatti RG, Leite KCE, Miranda GHB, Rodrigues FHG. 2007. Evidence of high inbreeding in a population of the endangered giant anteater, *Myrmecophaga tridactyla* (Myrmecophagidae), from Emas National Park, Brazil. *Genetics and Molecular Biology* 30: 112-120.

Colwell RK, Chao A, Gotelli NJ, Lin S-Y, Mao CX, Chazdon RL, Longino JT. 2012. Models and estimators linking individual-based and sample-based rarefaction, extrapolation and comparison of assemblages. *Journal of Plant Ecology* 5: 3-21.

Coutinho M, Campos Z, Mourão G, Mauro R. 1997. Aspectos ecológicos dos vertebrados terrestres e semi-aquáticos no Pantanal. In: *Plano de conservação da Bacia do Alto Paraguai. Diagnósticos dos meios físico e biótico: meio biótico*. Brasília: Ministério do Meio Ambiente, dos Recursos Hídricos e da Amazônia Legal, 183-322.

Cunha HF, Moreira FGA, Silva SS. 2010. Roadkill of wild vertebrates along the GO-060 road between Goiânia and Iporá, Goiás State, Brazil. *Acta Scientiarum. Biological Sciences*. 32: 257-263.

Desbiez ALJ, Medri IM. 2010. Density and habitat use by giant anteaters (*Myrmecophaga tridactyla*) and southern tamanduas (*Tamandua tetradactyla*) in the Pantanal wetland, Brazil. *Edentata* 11: 4-10.

Di Blanco YE, Pérez IJ, Di Bitetti MS. 2015. Habitat selection in reintroduced giant anteaters: the critical role of conservation areas. *Journal of Mammalogy* 96: 1024-1035.

Di Blanco YE, Desbiez ALJ, Jiménez-Pérez I, Kluyber D, Massocato GF, Di Bitetti MS. 2017. Habitat selection and home-range use by resident and reintroduced giant anteaters in 2 South American wetlands. *Journal of Mammalogy* 98: 1118-1128.

Diniz MF, Brito D. 2015. Protected areas effectiveness in maintaining viable giant anteater (*Myrmecophaga tridactyla*) populations in an agricultural frontier. *Natureza & Conservação* 13: 145-151.

Douzery E, Randi E. 1997. The mitochondrial control region of Cervidae: evolutionary patterns and phylogenetic content. *Molecular Biology and Evolution* 14: 1154-1166.

Eisenberg JF, O'Connell MA, August PV. 1979. Density, productivity and distribution of mammals in two Venezuelan habitats. In: Eisenberg JF, ed. *Vertebrate ecology in the northern neotropics*. Washington, DC: Smithsonian Institution Press, 187-207.

Eizirik E, Kim JH, Menotti-Raymond M, Crawshaw Jr. PG, O'Brien SJ, Johnson WE. 2001. Phylogeography, population history and conservation genetics of jaguars (*Panthera onca*, Mammalia, Felidae). *Molecular Ecology* 10: 65-79.

Excoffier L, Lischer HEL. 2010. Arlequin suite ver 3.5: a new series of programs to perform population genetics analyses under Linux and Windows. *Molecular Ecology Resources* 10: 564-567.

Excoffier L, Smouse PE, Quattro JM. 1992. Analysis of molecular variance inferred from metric distances among DNA haplotypes: application to human mitochondrial DNA restriction data. *Genetics* 131: 479-491.

Figel JJ, Botero-Cañola S, Sánchez-Londoño JD, Quintero-Ángel A. 2015. Unexpected documentation and inter-Andean range expansion of a vulnerable large mammal (Mammalia, Pilosa, *Myrmecophaga tridactyla*) in Colombia. *Mammalia* 80: 449-452.

Flot JF. 2010. SeqPHASE: a web tool for interconverting PHASE input/output files and FASTA sequence alignments. *Molecular Ecology Resources* 10: 162-166.

Françoso RD, Brandão R, Nogueira CC, Salmona YB, Machado RB, Colli GR. 2015. Habitat loss and the effectiveness of protected areas in the Cerrado Biodiversity Hotspot. *Natureza & Conservação* 13: 35-40.

Frankham R. 2005. Genetics and extinction. *Biological Conservation* 126: 131-140.

Freitas CH, Justino CS, Setz EZF. 2014. Road-kills of the giant anteater in south-eastern Brazil: 10 years monitoring spatial and temporal determinants. *Wildlife Research* 41: 673-680.

Frutos SD, Van Den Bussche RA. 2002. Genetic diversity and gene flow in nine-banded armadillos in Paraguay. *Journal of Mammalogy* 83: 815-823.

Garcia JE, Vilas Boas LA, Lemos MVF, Lemos EGM, Contel EPB. 2005. Identification of microsatellite DNA markers for the giant anteater *Myrmecophaga tridactyla*. *Journal of Heredity* 96: 600-602.

Gardner AL. 2007. Suborder Vermilingua. In: Gardner AL, ed. *Mammals of South America, volume 1: marsupials, xenarthrans, shrews, and bats*. Chicago, IL: University of Chicago Press, 168-177.

Gibb GC, Condamine FL, Kuch M, Enk J, Moraes-Barros N, Superina M, Poinar HN, Delsuc F. 2016. Shotgun mitogenomics provides a reference phylogenetic framework and timescale for living xenarthrans. *Molecular Biology and Evolution* 33: 621-642.

Gotelli NJ, Colwell RK. 2011. Estimating species richness. In: Magurran AE, McGill BJ, eds. *Frontiers in measuring biodiversity*. New York, NY: Oxford University Press, 39-54.

Guillot G. 2008. Inference of structure in subdivided populations at low levels of genetic differentiation - the correlated allele frequencies model revisited. *Bioinformatics* 24: 2222-2228.

Guillot G, Mortier F, Estoup A. 2005. Geneland: a computer package for landscape genetics. *Molecular Ecology Notes* 5: 708-711.

Guillot G, Estoup A, Mortier F, Cosson JF. 2005. A spatial statistical model for landscape genetics. *Genetics* 170: 1261-1280.

Guillot G, Santos F, Estoup A. 2008. Analysing georeferenced population genetics data with Geneland: a new algorithm to deal with null alleles and a friendly graphical user interface. *Bioinformatics* 24: 1406-1407.

Haffer J. 1969. Speciation in Amazonian forest birds. *Science* 165: 131-137.

Harris MB, Tomas W, Mourão G, Silva CJ, Guimarães E, Sonoda F, Fachim E. 2005. Safeguarding the Pantanal wetlands: threats and conservation initiatives. *Conservation Biology* 19: 714-720.

Heled J, Drummond AJ. 2008. Bayesian inference of population size history from multiple loci. *BMC Evolutionary Biology* 8(289).

Heller R, Chikhi L, Siegismund HR. 2013. The confounding effect of population structure on Bayesian skyline plot inferences of demographic history. *PLoS One* 8: e62992.

Hsieh TC, Ma KH, Chao A. 2016. iNEXT: an R package for rarefaction and extrapolation of species diversity (Hill numbers). *Methods in Ecology and Evolution* 7: 1451-1456.

Huchon D, Delsuc F, Catzeflis FM, Douzery EJP. 1999. Armadillos exhibit less genetic polymorphism in North America than in South America: nuclear and mitochondrial data confirm a founder effect in *Dasypus novemcinctus* (Xenarthra). *Molecular Ecology* 8: 1743-1748.

Kimura M. 1980. A simple method for estimating evolutionary rates of base substitutions through comparative studies of nucleotide sequences. *Journal of Molecular Evolution* 16: 111-120.

Klink CA, Machado RB. 2005. Conservation of the Brazilian Cerrado. *Conservation Biology* 19: 707-713.

Kreutz K, Fischer F, Linsenmair KE. 2012. Timber plantations as favourite habitat for giant anteaters. *Mammalia* 76: 137-142.

Kumar S, Stecher G, Tamura K. 2016. MEGA7: molecular evolutionary genetics analysis version 7.0 for bigger datasets. *Molecular Biology and Evolution* 33: 1870-1874.

Lara-Ruiz P, Chiarello AG, Santos FR. 2008. Extreme population divergence and conservation implications for the rare endangered Atlantic Forest sloth, *Bradypus torquatus* (Pilosa: Bradypodidae). *Biological Conservation* 141: 1332-1342.

Leeuwenberg F. 1997. Edentata as a food resource: subsistence hunting by Xavante Indians, Brazil. *Edentata* 3: 4-5.

Leigh JW, Bryant D. 2015. PopART: full-feature software for haplotype network construction. *Methods in Ecolology and Evolution* 6: 1110-1116.

Macedo LSM. 2008. Área de vida, atividade, uso de habitat e padrões hematológicos de tamanduá-bandeira (*Myrmecophaga tridactyla*, Linnaeus 1758) nas savanas periurbanas de Boa Vista, Roraima. Unpublished M. Sc. Thesis, Universidade Federal de Roraima.

Macedo LSM, Azevedo RB, Pinto F. 2010. Área de vida, uso do habitat e padrão de atividade do tamanduá-bandeira na savana de Boa Vista, Roraima. In: Barbosa RI, Melo VF, eds. *Roraima: homem, ambiente e ecologia*. Boa Vista, RR: Femact, 585-601.

Magalhães RF, Lemes P, Camargo A, Oliveira U, Brandão RA, Thomassen H, Garcia PCA, Leite FSF, Santos FR. 2017. Evolutionarily significant units of the critically endangered leaf frog *Pithecopus ayeaye* (Anura, Phyllomedusidae) are not effectively preserved by the Brazilian protected areas network. *Ecology and Evolution* in press.

Medri IM, Mourão G. 2005. Home range of giant anteaters (*Myrmecophaga tridactyla*) in the Pantanal wetland, Brazil. *Journal of Zoology* 266: 365-375.

Medri IM, Mourão GM, Rodrigues FHG. 2011. Ordem Pilosa. In: Reis NR, Peracchi AL, Pedro WA, Lima IP, eds. *Mamíferos do Brasil.* 2nd edition. Londrina, PR: Reis NR, 91-106.

Meirmans PG. 2015. Seven common mistakes in population genetics and how to avoid them. *Molecular Ecology* 24: 3223-3231.

Meritt DA. 2008. Xenarthrans of the Paraguayan Chaco. Em: Vizcaino SF, Loughry WJ, eds. *The biology of the Xenarthra*. Gainesville, FL: University Press of Florida, 294-299.

Miller MP. 2005. Alleles In Space (AIS): computer software for the joint analysis of interindividual spatial and genetic information. *Journal of Heredity* 96: 722-724.

Miller MA, Pfeiffer W, Schwartz T. 2010. Creating the CIPRES Science Gateway for inference of large phylogenetic trees. New Orleans, LA: Proceedings of the Gateway Computing Environments Workshop, 1-8.

Miranda F, Bertassoni A, Abba AM. 2014. *Myrmecophaga tridactyla*. The IUCN red list of threatened species 2014: e.T14224A47441961.

Miranda GHB. 2004. Ecologia e conservação do tamanduá-bandeira (*Myrmecophaga tridactyla* Linnaeus, 1758) no Parque Nacional das Emas. Unpublished D. Phil. Thesis, Universidade de Brasília.

Miranda GHB, Tomás WM, Valladares-Pádua CB, Rodrigues FHG. 2006. Giant anteater (*Myrmecophaga tridactyla*) population survey in Emas National Park, Brazil - a proposed monitoring program. *Endangered Species UPDATE* 23: 96-103.

Montgomery GG, Lubin YD. 1977. Prey influences on movements of Neotropical anteaters. In: Phillips RL, Jonkel C, eds. *Proceedings of the 1975 predator symposium*. Missoula, MT: Montana Forest and Conservation Experiment Station, University of Montana, 103-131.

Mourão G, Medri IM. 2007. Activity of a specialized insectivorous mammal (*Myrmecophaga tridactyla*) in the Pantanal of Brazil. *Journal of Zoology* 271: 187-192.

Murphy WJ, Eizirik E, Johnson WE, Zhang YP, Ryder OA, O'Brien SJ. 2001. Molecular phylogenetics and the origins of placental mammals. *Nature* 409: 614-618.

Naples VL. 1999. Morphology, evolution and function of feeding in the giant anteater (*Myrmecophaga tridactyla*). *Journal of Zoology* 249: 19-41.

Nardelli M, Ibáñez EA, Dobler D, Justy F, Delsuc F, Abba AM, Cassini MH, Túnez JI. 2016. Genetic structuring in a relictual population of screaming hairy armadillo (*Chaetophractus vellerosus*) in Argentina revealed by a set of novel microsatellite loci. *Genetica* 144: 469-476.

Noss AJ, Cuéllar RL, Cuéllar E. 2008. Exploitation of Xenarthrans by the Guaraní-Isoseño indigenous people of the Bolivian Chaco: comparisons with hunting by other indigenous groups in Latin America, and implications for conservation. Em: Vizcaino SF, Loughry WJ, eds. *The biology of the Xenarthra*. Gainesville, FL: University Press of Florida, 244-254.

Prado JL, Martinez-Maza C, Alberdi MT. 2015. Megafauna extinction in South America: a new chronology for the Argentine Pampas. *Palaeogeography, Palaeoclimatology, Palaeoecology* 425: 41-49.

Quiroga VA, Noss AJ, Boaglio GI, Di Bitetti MS. 2016. Local and continental determinants of giant anteater (*Myrmecophaga tridactyla*) abundance: biome, human and jaguar roles in population regulation. *Mammalian Biology* 81: 274-280.

R Core Team. 2017. *R: a language and environment for statistical computing*. Vienna, Austria: R Foundation for Statistical Computing. Available at: https://www.R-project.org/.

Rambaut A, Suchard MA, Xie D, Drummond AJ. 2014. Tracer v.1.6. Available at: http://beast.bio.ed.ac.uk/Tracer.

Redford KH. 1994. The edentates of the Cerrado. *Edentata* 1: 4-10.

Ribeiro MC, Metzger JP, Martensen AC, Ponzoni FJ, Hirota MM. 2009. The Brazilian Atlantic Forest: how much is left, and how is the remaining forest distributed? Implications for conservation. *Biological Conservation* 142: 1141-1153.

Rojano C, Miranda L, Ávila R. 2015. Densidad poblacional y biomasa del oso hormiguero gigante (*Myrmecophaga tridactyla*) en Pore, Casanare, Colombia. *Revista Biodiversidad Neotropical* 5: 64-70.

Rojano CB, Giraldo MEL, Miranda-Cortés L, Avilán RA. 2015. Área de vida y uso de hábitats de dos individuos de oso palmero (*Myrmecophaga tridactyla*) en Pore, Casanare, Colombia. *Edentata* 16: 37-45.

Sambrook J, Russell DW. 2001. *Molecular cloning: a laboratory manual*. 3rd edition. Cold Spring Harbor, NY: Cold Spring Harbor Laboratory Press.

Santos Júnior JE, Santos FR, Silveira FA. 2015. Hitting an unintended target: phylogeography of *Bombus brasiliensis* Lepeletier, 1836 and the first new Brazilian bumblebee species in a century (Hymenoptera: Apidae). *PLoS One* 10: e0125847.

Schetino MAA, Coimbra RTF, Santos FR. 2017. Time scaled phylogeography and demography of *Bradypus torquatus* (Pilosa: Bradypodidae). *Global Ecology and Conservation* 11: 224-235.

Shaw JH, Carter TS, Machado-Neto J. 1985. Ecology of the giant anteater *Myrmecophaga tridactyla* in Serra da Canastra, Minas Gerais, Brazil: a pilot study. In: Montgomery GG,ed. *The evolution and ecology of armadillos, sloths, and vermilinguas*. Washington, DC: Smithsonian Institution Press, 379-384.

Shaw JH, Machado-Neto J, Carter TS. 1987. Behavior of free-living giant anteaters (*Myrmecophaga tridactyla*). *Biotropica* 19: 255-259.

Silva MP, Mauro R, Mourão G, Coutinho M. 2000. Distribuição e quantificação de classes de vegetação do Pantanal através de levantamento aéreo. *Revista Brasileira de Botânica* 23: 143-152.

Silveira L, Rodrigues FHG, Jácomo ATA, Diniz Filho JAF. 1999. Impacts of wildfires on the megafauna of the Emas National Park, central Brazil. *Oryx* 33: 108-114.

Stephens M, Scheet P. 2005. Accounting for decay of linkage disequilibrium in haplotype inference and missing-data imputation. *American Journal of Human Genetics* 76: 449-462.

Stephens M, Smith NJ, Donnelly P. 2001. A new statistical method for haplotype reconstruction from population data. *American Journal of Human Genetics* 68: 978-989.

Tavaré S. 1986. Some probabilistic and statistical problems in the analysis of DNA sequences. In: Miura RM, ed. *Some mathematical questions in biology: DNA sequence analysis. Lectures on mathematics in the life sciences, volume 17.* Providence, RI: American Mathematical Society, 57-86.

Teeling EC, Scally M, Kao DJ, Romagnoli ML, Springer MS, Stanhope MJ. 2000. Molecular evidence regarding the origin of echolocation and flight in bats. *Nature* 403: 188-192.

Thompson JD, Higgins DG, Gibson TJ. 1994. Clustal W: improving the sensitivity of progressive multiple sequence alignment through sequence weighting, position-specific gap penalties and weight matrix choice. *Nucleic Acids Research* 22: 4673-4680.

Villavicencio NA, Lindsey EL, Martin FM, Borrero LA, Moreno PI, Marshall CR, Barnosky AD. 2016. Combination of humans, climate, and vegetation change triggered Late Quaternary megafauna extinction in the Última Esperanza region, southern Patagonia, Chile. *Ecography* 39: 125-140.

Vynne C, Keim JL, Machado RB, Marinho-Filho J, Silveira L, Groom MJ, Wasser SK. 2011. Resource selection and its implications for wide-ranging mammals of the Brazilian Cerrado. *PLoS One* 6: e28939.

Wang IJ, Bradburd GS. 2014. Isolation by environment. *Molecular ecology* 23: 5649-5662.

Ward RH, Frazier BL, Dew-Jager K, Pääbo S. 1991. Extensive mitochondrial diversity within a single Amerindian tribe. *Proceedings of the National Academy of Sciences of the United States of America* 88: 8720-872.

Werneck FP, Nogueira C, Colli GR, Sites Jr JW, Costa GC. 2012. Climatic stability in the Brazilian Cerrado: implications for biogeographical connections of South American savannas, species richness and conservation in a biodiversity hotspot. *Journal of Biogeography* 39: 1695-1706.

Wetzel RM. 1982. Systematics, distribution, ecology, and conservation of South American edentates. In: Mares MA, Genoways HH, eds. *Pymatuning Symposia in Ecology, volume 6: mammalian biology in South America*. Linesville, PA: University of Pittsburgh, 345-375.

Whitlock MC, McCauley DE. 1999. Indirect measures of gene flow and migration: $F_{ST} \neq 1/(4Nm+1)$. *Heredity* 82: 117-125.

Zimbres BQC, Aquino PPU, Machado RB, Silveira L, Jácomo ATA, Sollmann R, Tôrres NM, Furtado MM, Marinho-Filho J. 2012. Range shifts under climate change and the role of protected areas for armadillos and anteaters. *Biological Conservation* 152: 53-61.

Zimbres B, Furtado MM, Jácomo ATA, Silveira L, Sollmann R, Tôrres NM, Machado RB, Marinho-Filho J. 2013. The impact of habitat fragmentation on the ecology of xenarthrans (Mammalia) in the Brazilian Cerrado. *Landscape Ecology* 28: 259-269.

7. Figures

Figure 1. Map produced with ArcGIS v10.4 showing the sampling localities. Atlantic Forest (AF and ▲); Amazonia (AM and ♦); Cerrado (CE and ●); and Pantanal (PT and ■).

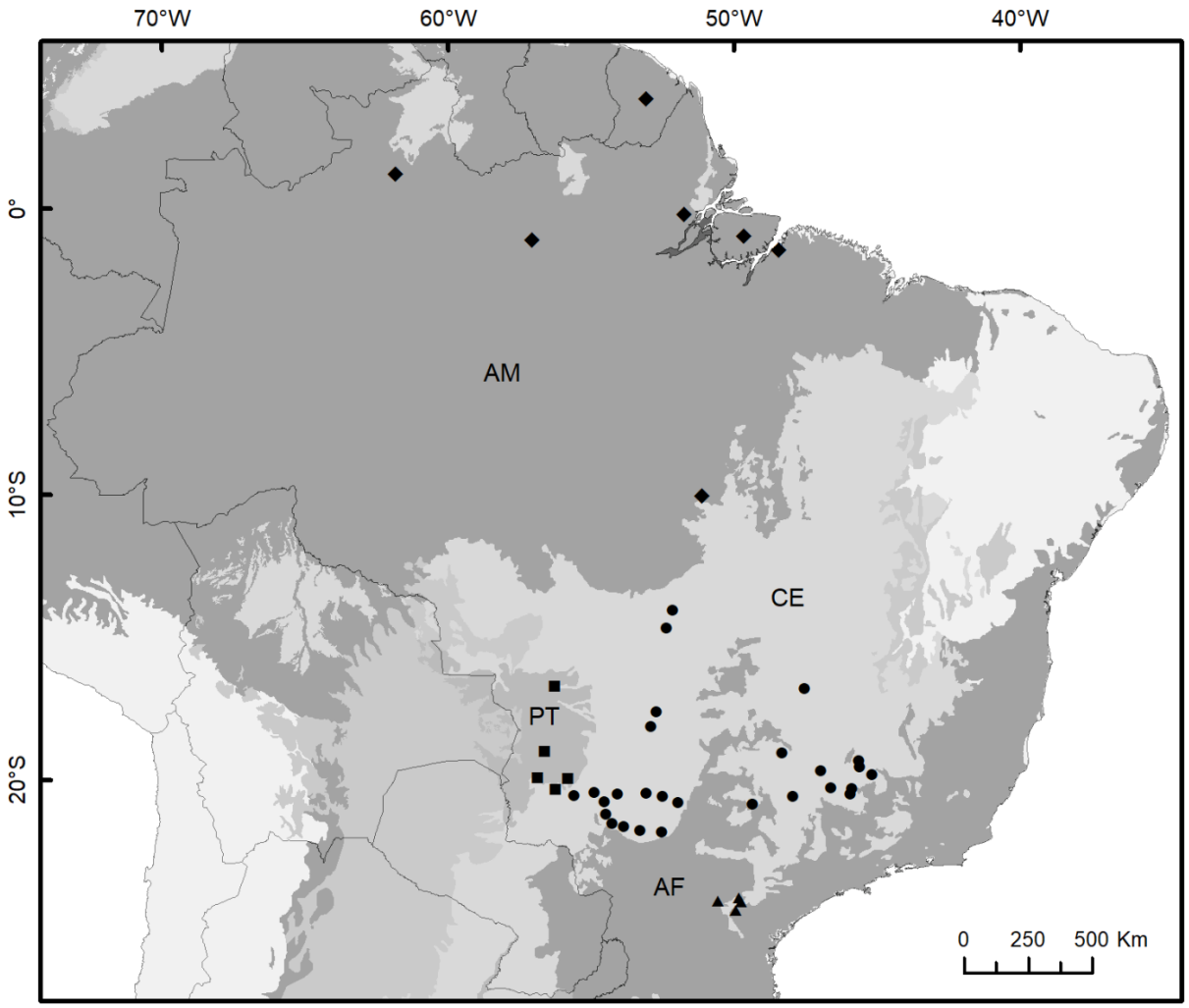

Figure 2. Scheme of the different scenarios (**I-V**) used for model testing in Migrate-n. Populations represent the Geneland clusters and are abbreviated as follows: Amazonia [AM] and Cerrado+Pantanal+Atlantic Forest [CEPTAF]. Dotted line delimits (**I**) a single panmictic population; dashed lines represent (**II-IV**) populations experiencing gene flow; and solid lines depicts (**V**) isolated populations. Arrows show the direction of migration.

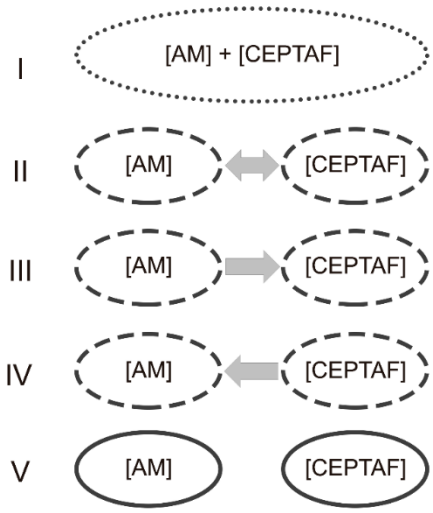

Figure 3. Median-joining haplotype networks for (**A**) concatenated mtDNA segments, (**B**) exon 28 of vWF, (**C**) BDNF and (**D**) RAG2. Circles represent haplotypes and color represent biomes. Hatch marks symbolizes mutations.

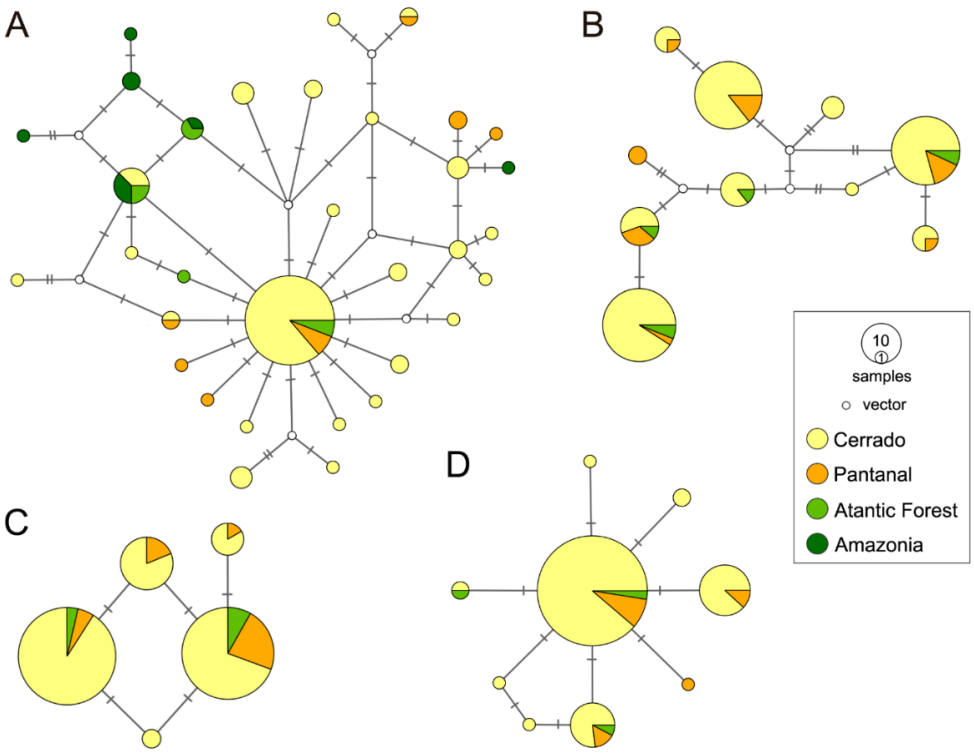

Figure 4. Geneland results showing (**A**) a plot with the probability densities for each number of clusters assessed and (**B**) a map with posterior probabilities of membership for the two most likely clusters: Amazonia [AM] and Cerrado+Pantanal+Atlantic Forest [CEPTAF].

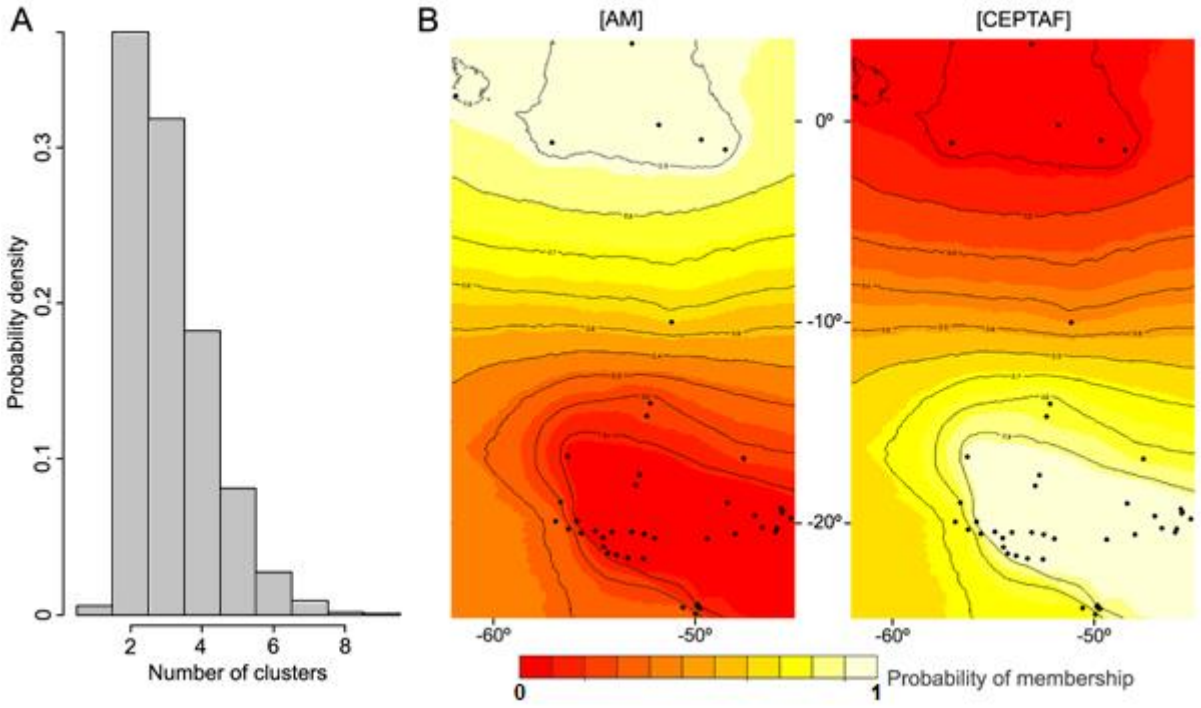

Figure 5. Interindividual Mantel test graph showing a slight correlation (r = 0.1213 and P = 0.0040) between $\log_{10}$-transformed genetic and geographic distances.

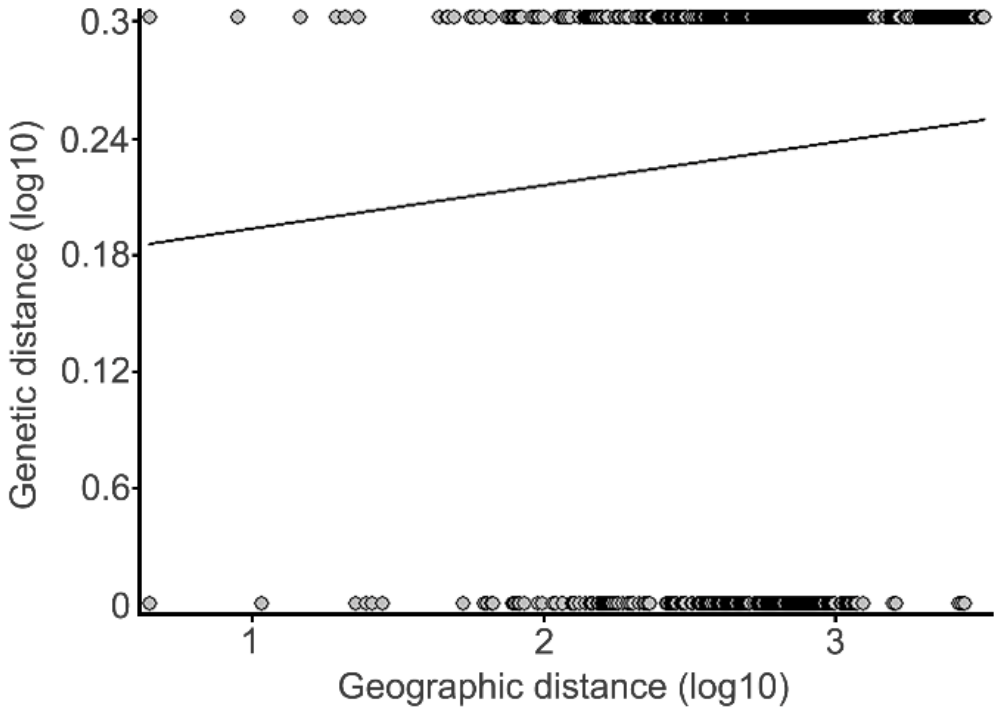

Figure 6. Rarefaction/extrapolation haplotypes richness curves for the two populations identified by Geneland: Amazonia [AM] and Cerrado+Pantanal+Atlantic Forest [CEPTAF]. Three types of curves are shown: (**A**) a sample size-based, (**B**) a sample completeness and (**C**) a coverage-based. Solid lines are result of interpolation and dashed lines represent extrapolation. Lighter areas around the asymptote delimit the 95% confidence intervals. ● = [AM], and ▲ = [CEPTAF].

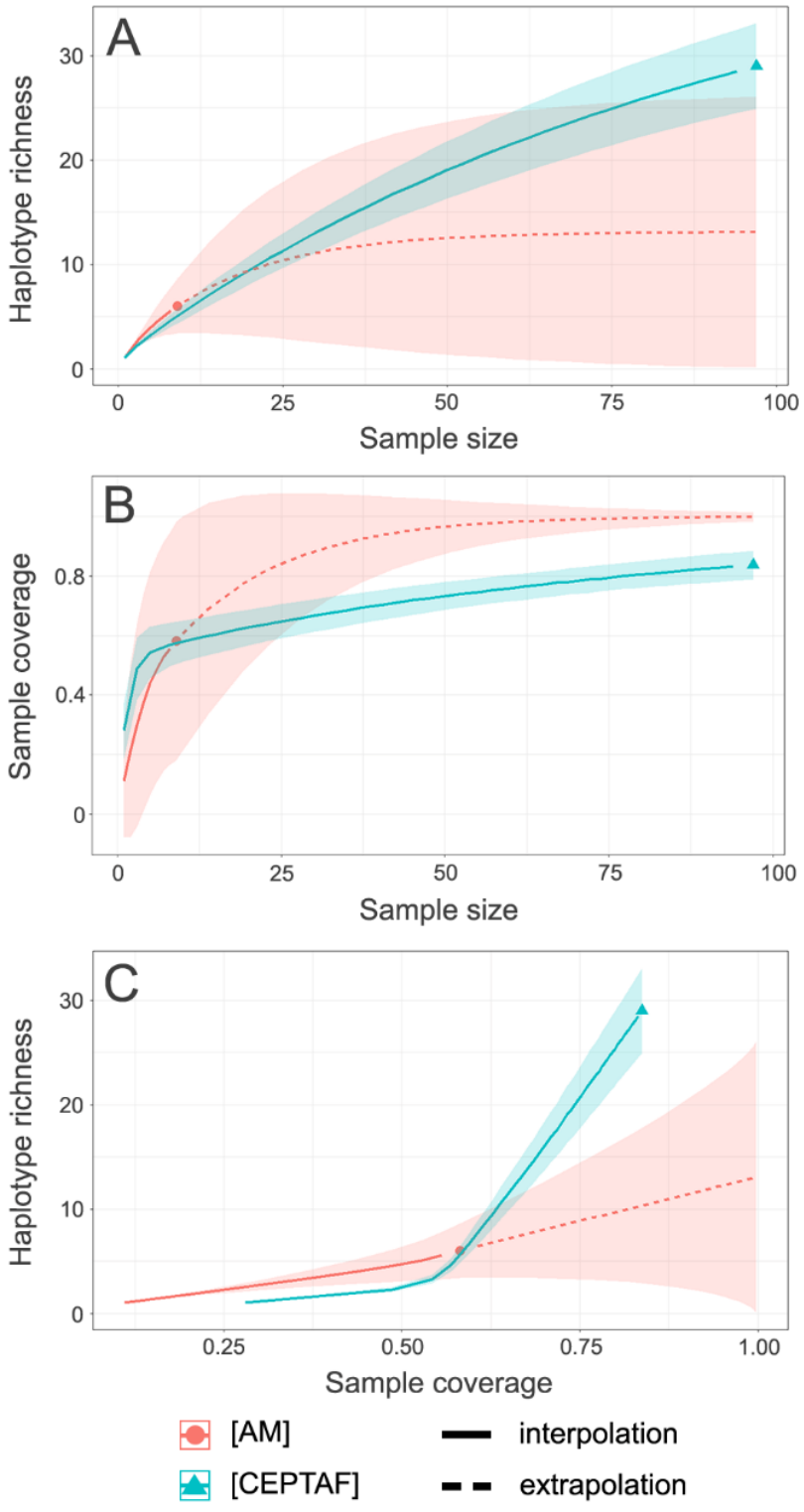

Figure 7. Extended Bayesian skyline plot for *M. tridactyla*. The analysis was calibrated with an estimated Cytb clock rate of 7.4513 x 10^{-3} substitutions/site/million years. The plot shows a population growth that starts slowly at ca. 60 kya and largely increases since ca. 40 kya, reaching a present population size of ~ 7.5 times the size of the ancestral population. The dashed line represents the median estimate and the grey area around it corresponds to the 95% central posterior density (CPD).

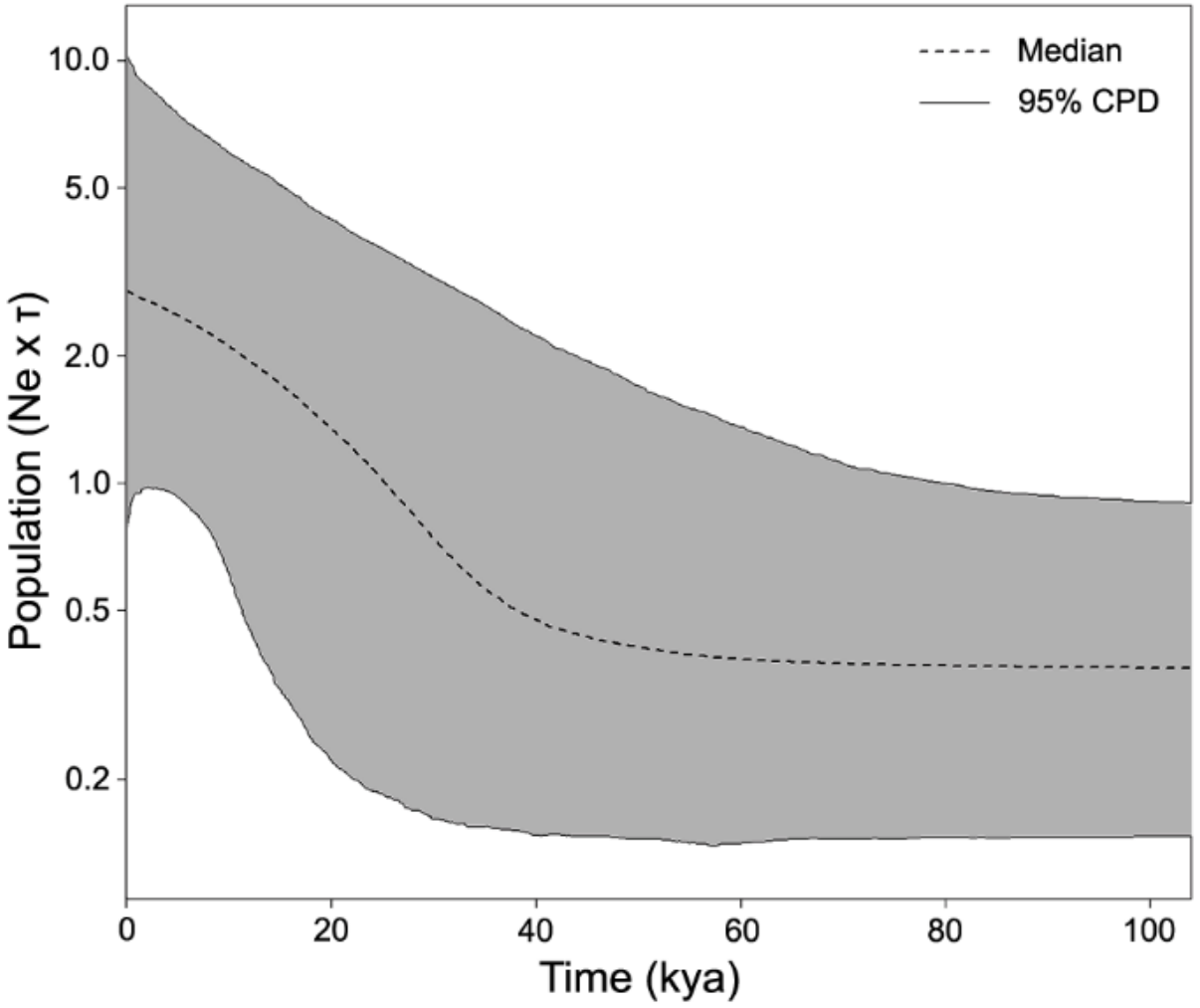

8. Tables

Table 1. List of primers used for each marker in this work and their references.

Locus	Pairs of primers (5' - 3')		References
HVI	L0: CCCAAAGCTGAAATTCTACTTAAACTA		Douzery & Randi, 1997
	E3: ATGACCCTGAAGAAASAACCAG		Huchon et al., 1999
	ProL: ATTACACTGGTCTTGTAAACC		LBEM
	H16498: CCTGAAGTAGGAACCAGATG		Ward et al., 1991
Cytb	Cytb-L: CCATGAGGACAAATATCATTCTGAGG		Coimbra et al., 2017
	Cytb-H: TGGTTTACAAGACCAGTGTAAT		
RAG2	F220: GATTCCTGCTAYCTYCCTCCTCT	external	Teeling et al., 2000
	R995: CCCATGTTGCTTCCAAACCATA		
	TCATGGAGGGAAAACACCAAA	internal	Murphy et al., 2001
	TGCACTGGAGACAGAGATTC		
vWF	vWF1F: TGTCAACCTCACCTGTGAAGCCTG		Schetino et al., 2017
	vWF1R: TGCAGGACCAGGTCAGGAGCCTCTC		
BDNF	CATCCTTTTCCTTACTATGGTT		Murphy et al., 2001
	TTCCAGTGCCTTTTGTCTATG		

Table 2. Summary of the concatenated mtDNA genetic diversity parameters estimated for each population with the Kimura-2P model. N = number of samples; H = number of haplotypes; h = haplotype diversity; and π = nucleotide diversity.

Population	N	H	h (σ)	π (σ)
[AM]	9	6	0.8889 ± 0.0910	0.0027 ± 0.0018
[CEPTAF]	97	29	0.7204 ± 0.0512	0.0019 ± 0.0012
Total	106	33	0.7623 ± 0.0445	0.0021 ± 0.0013

Table 3. Migrate-n model selection through Bayes factors. Bézier approximation scores and probabilities for each model are shown. Numerals I-V correspond to models in Figure 2.

Model	Description	Bézier approximation score	Probability
I	Panmixia	-1901.6788	0.0000
II	Bidirectional migration	-1892.3102	0.0891
III	Migration from [AM] to [CEPTAF]	-1890.0575	0.8476
IV	Migration from [CEPTAF] to [AM]	-1892.6514	0.0633
V	Isolated populations	-1927.6109	0.0000

9. Supporting information

Table S1. List of samples and sampling localities contained in this work. Coordinates for localities marked with a * are rough approximations. AM = Amazonia; CE = Cerrado; PT = Pantanal; and AF = Atlantic Forest.

Sample ID	Country	State	Locality	Biome	Longitude	Latitude
MPEG01652	Brazil	Amapá	Mazagão*	AM	51°43'56.80"W	00°11'02.46"S
MPEG01662	Brazil	Amapá	Mazagão*	AM	51°43'56.80"W	00°11'02.46"S
M0681	Brazil	Goiás	Cristalina*	CE	47°31'53.97"W	16°47'40.70"S
M1683	Brazil	Goiás	Mineiros	CE	52°42'16.92"W	17°36'37.08"S
Filhote	Brazil	Goiás	Emas National Park*	CE	52°54'54.32"W	18°07'17.86"S
TBC01	Brazil	Goiás	Emas National Park*	CE	52°54'54.32"W	18°07'17.86"S
TBC02	Brazil	Goiás	Emas National Park*	CE	52°54'54.32"W	18°07'17.86"S
TBC03	Brazil	Goiás	Emas National Park*	CE	52°54'54.32"W	18°07'17.86"S
TBC04	Brazil	Goiás	Emas National Park*	CE	52°54'54.32"W	18°07'17.86"S
TBC06	Brazil	Goiás	Emas National Park*	CE	52°54'54.32"W	18°07'17.86"S
TBC07	Brazil	Goiás	Emas National Park*	CE	52°54'54.32"W	18°07'17.86"S
TBC08	Brazil	Goiás	Emas National Park*	CE	52°54'54.32"W	18°07'17.86"S
TBC09	Brazil	Goiás	Emas National Park*	CE	52°54'54.32"W	18°07'17.86"S
TBC10	Brazil	Goiás	Emas National Park*	CE	52°54'54.32"W	18°07'17.86"S
TBC11	Brazil	Goiás	Emas National Park*	CE	52°54'54.32"W	18°07'17.86"S
TBC12	Brazil	Goiás	Emas National Park*	CE	52°54'54.32"W	18°07'17.86"S
TBC13	Brazil	Goiás	Emas National Park*	CE	52°54'54.32"W	18°07'17.86"S
TBC15	Brazil	Goiás	Emas National Park*	CE	52°54'54.32"W	18°07'17.86"S
TBC16	Brazil	Goiás	Emas National Park*	CE	52°54'54.32"W	18°07'17.86"S
TBC17	Brazil	Goiás	Emas National Park*	CE	52°54'54.32"W	18°07'17.86"S

TBC20	Brazil	Goiás	Emas National Park*	CE	52°54'54.32"W	18°07'17.86"S
TBC21	Brazil	Goiás	Emas National Park*	CE	52°54'54.32"W	18°07'17.86"S
TBC22	Brazil	Goiás	Emas National Park*	CE	52°54'54.32"W	18°07'17.86"S
TBC23	Brazil	Goiás	Emas National Park*	CE	52°54'54.32"W	18°07'17.86"S
TBC24	Brazil	Goiás	Emas National Park*	CE	52°54'54.32"W	18°07'17.86"S
TBC25	Brazil	Goiás	Emas National Park*	CE	52°54'54.32"W	18°07'17.86"S
TBC26	Brazil	Goiás	Emas National Park*	CE	52°54'54.32"W	18°07'17.86"S
TBC28	Brazil	Goiás	Emas National Park*	CE	52°54'54.32"W	18°07'17.86"S
TBC29	Brazil	Goiás	Emas National Park*	CE	52°54'54.32"W	18°07'17.86"S
TBC30	Brazil	Goiás	Emas National Park*	CE	52°54'54.32"W	18°07'17.86"S
TBC31	Brazil	Goiás	Emas National Park*	CE	52°54'54.32"W	18°07'17.86"S
M0668	Brazil	Minas Gerais	Araxá*	CE	46°58'05.00"W	19°39'07.31"S
M2004	Brazil	Minas Gerais	Bom Despacho	CE	45°10'34.30"W	19°47'12.10"S
M0985	Brazil	Minas Gerais	Dores do Indaiá	CE	45°36'49.70"W	19°31'04.60"S
M2008	Brazil	Minas Gerais	Dores do Indaiá	CE	45°34'19.70"W	19°26'12.10"S
M0986	Brazil	Minas Gerais	Doresópolis*	CE	45°52'52.43"W	20°17'35.27"S
M0707	Brazil	Minas Gerais	Piumhi	CE	45°56'45.00"W	20°27'42.00"S
M1776	Brazil	Minas Gerais	Quartel Geral	CE	45°38'51.10"W	19°18'36.00"S
M2146	Brazil	Minas Gerais	Uberlândia*	CE	48°20'03.31"W	19°01'44.18"S
TBR	Brazil	Minas Gerais	Uberlândia*	CE	48°20'03.31"W	19°01'44.18"S
M0663	Brazil	Minas Gerais	Serra da Canastra National Park*	CE	46°37'21.39"W	20°15'09.69"S
M0712	Brazil	Minas Gerais	Serra da Canastra National Park*	CE	46°37'21.39"W	20°15'09.69"S
SCMT01	Brazil	Minas Gerais	Serra da Canastra National Park*	CE	46°37'21.39"W	20°15'09.69"S
SCMT02	Brazil	Minas Gerais	Serra da Canastra National Park*	CE	46°37'21.39"W	20°15'09.69"S
SCMT03	Brazil	Minas Gerais	Serra da Canastra National Park*	CE	46°37'21.39"W	20°15'09.69"S
SCMT04	Brazil	Minas Gerais	Serra da Canastra National Park*	CE	46°37'21.39"W	20°15'09.69"S

SCMT05	Brazil	Minas Gerais	Serra da Canastra National Park*	CE	46°37'21.39"W	20°15'09.69"S
SCMT06	Brazil	Minas Gerais	Serra da Canastra National Park*	CE	46°37'21.39"W	20°15'09.69"S
SCMT07	Brazil	Minas Gerais	Serra da Canastra National Park*	CE	46°37'21.39"W	20°15'09.69"S
SCMT08	Brazil	Minas Gerais	Serra da Canastra National Park*	CE	46°37'21.39"W	20°15'09.69"S
SCMT09	Brazil	Minas Gerais	Serra da Canastra National Park*	CE	46°37'21.39"W	20°15'09.69"S
SCMT10	Brazil	Minas Gerais	Serra da Canastra National Park*	CE	46°37'21.39"W	20°15'09.69"S
SCMT11	Brazil	Minas Gerais	Serra da Canastra National Park*	CE	46°37'21.39"W	20°15'09.69"S
SCMT12	Brazil	Minas Gerais	Serra da Canastra National Park*	CE	46°37'21.39"W	20°15'09.69"S
SCMT13	Brazil	Minas Gerais	Serra da Canastra National Park*	CE	46°37'21.39"W	20°15'09.69"S
SCMT15	Brazil	Minas Gerais	Serra da Canastra National Park*	CE	46°37'21.39"W	20°15'09.69"S
LabBMC0012	Brazil	Mato Grosso do Sul	Anastácio	CE	55°36'07.00"W	20°31'15.00"S
FRM05	Brazil	Mato Grosso do Sul	Aquidauana*	PT	55°49'04.04"W	19°56'02.45"S
LabBMC0135	Brazil	Mato Grosso do Sul	Bataguassu	CE	52°31'07.00"W	21°47'37.00"S
LabBMC0083	Brazil	Mato Grosso do Sul	Campo Grande	CE	54°32'01.00"W	20°45'05.00"S
M0697	Brazil	Mato Grosso do Sul	Corumbá*	PT	56°37'19.00"W	18°59'11.00"S
M0698	Brazil	Mato Grosso do Sul	Corumbá*	PT	56°37'19.00"W	18°59'11.00"S
LabBMC0110	Brazil	Mato Grosso do Sul	Miranda	PT	56°51'40.00"W	19°54'44.00"S
LabBMC0124	Brazil	Mato Grosso do Sul	Miranda	PT	56°14'33.00"W	20°18'43.00"S
LabBMC0155	Brazil	Mato Grosso do Sul	Nova Alvorada do Sul	CE	54°28'23.00"W	21°10'39.00"S
LabBMC0281	Brazil	Mato Grosso do Sul	Nova Alvorada do Sul	CE	54°15'49.00"W	21°29'56.00"S
LabBMC0397	Brazil	Mato Grosso do Sul	Nova Alvorada do Sul	CE	53°51'03.00"W	21°36'02.00"S
LabBMC0168	Brazil	Mato Grosso do Sul	Nova Andradina	CE	53°16'39.00"W	21°44'52.00"S
LabBMC0007	Brazil	Mato Grosso do Sul	Ribas do Rio Pardo	CE	53°04'09.00"W	20°26'34.00"S
LabBMC0136	Brazil	Mato Grosso do Sul	Ribas do Rio Pardo	CE	54°03'51.00"W	20°28'00.00"S
LabBMC0144	Brazil	Mato Grosso do Sul	Terenos	CE	54°53'56.00"W	20°25'47.00"S
LabBMC0121	Brazil	Mato Grosso do Sul	Três Lagoas	CE	52°29'44.00"W	20°33'54.00"S

LabBMC0122	Brazil	Mato Grosso do Sul	Três Lagoas	CE	51°57'17.00"W	20°46'46.00"S
M1676	Brazil	Mato Grosso	Água Boa*	CE	52°09'30.96"W	14°03'00.00"S
FRM02	Brazil	Mato Grosso	Barão de Melgaço*	PT	56°16'02.24"W	16°42'17.25"S
FRM03	Brazil	Mato Grosso	Barão de Melgaço*	PT	56°16'02.24"W	16°42'17.25"S
FRM06	Brazil	Mato Grosso	Barão de Melgaço*	PT	56°16'02.24"W	16°42'17.25"S
M0682	Brazil	Mato Grosso	Barão de Melgaço*	PT	56°16'02.24"W	16°42'17.25"S
M0696	Brazil	Mato Grosso	Barão de Melgaço*	PT	56°16'02.24"W	16°42'17.25"S
M0980	Brazil	Mato Grosso	Barão de Melgaço*	PT	56°16'02.24"W	16°42'17.25"S
M0883	Brazil	Mato Grosso	Nova Xavantina*	CE	52°21'11.00"W	14°40'24.00"S
MTTA02	Brazil	Mato Grosso	Nova Xavantina*	CE	52°21'11.00"W	14°40'24.00"S
MTTA04	Brazil	Mato Grosso	Nova Xavantina*	CE	52°21'11.00"W	14°40'24.00"S
MTTA10	Brazil	Mato Grosso	Nova Xavantina*	CE	52°21'11.00"W	14°40'24.00"S
M0705	Brazil	Mato Grosso	Vila Rica*	AM	51°07'08.65"W	10°00'51.15"S
MPEG08887	Brazil	Pará	Belém*	AM	48°25'09.38"W	01°25'53.63"S
MPEG00565	Brazil	Pará	Ilha do Marajó*	AM	49°38'21.50"W	00°56'26.45"S
MPEG01246	Brazil	Pará	Ilha do Marajó*	AM	49°38'21.50"W	00°56'26.45"S
MPEG10211	Brazil	Pará	Oriximiná*	AM	57°02'41.93"W	01°04'47.88"S
M2017	Brazil	Paraná	Arapoti	AF	49°48'35.07"W	24°05'47.15"S
M2018	Brazil	Paraná	Arapoti	AF	49°49'35.97"W	24°09'02.68"S
FB01	Brazil	Paraná	Jaguariaíva	AF	49°43'21.44"W	24°14'33.83"S
FB02	Brazil	Paraná	Jaguariaíva	AF	49°43'21.44"W	24°14'33.83"S
M2019	Brazil	Paraná	Jaguariaíva	AF	49°40'44.04"W	24°14'31.11"S
M1677	Brazil	Paraná	Piraí do Sul	AF	49°55'40.25"W	24°32'23.33"S
M0977	Brazil	Paraná	Telêmaco Borba*	AF	50°33'26.00"W	24°12'42.00"S
M1678	Brazil	Paraná	Telêmaco Borba	AF	50°33'26.00"W	24°12'42.00"S
MPEG01741	Brazil	Roraima	Caracaraí	AM	61°50'42.62"W	01°14'40.33"N

M2023	Brazil	São Paulo	São Joaquim da Barra*	CE	47°55'45.76"W	20°32'52.86"S
M0680	Brazil	São Paulo	São José do Rio Preto*	CE	49°20'40.00"W	20°48'49.00"S
M0684	Brazil	São Paulo	São José do Rio Preto*	CE	49°20'40.00"W	20°48'49.00"S
M0685	Brazil	São Paulo	São José do Rio Preto*	CE	49°20'40.00"W	20°48'49.00"S
M0686	Brazil	São Paulo	São José do Rio Preto*	CE	49°20'40.00"W	20°48'49.00"S
M0687	Brazil	São Paulo	São José do Rio Preto*	CE	49°20'40.00"W	20°48'49.00"S
M0693	Brazil	São Paulo	São José do Rio Preto*	CE	49°20'40.00"W	20°48'49.00"S
KT818549	French Guiana*			AM	53°04'55.23"W	03°51'37.05"N

Table S2. Summary of parameter estimates for each model tested in Migrate-n. We report the mode and the 95% highest posterior density (HPD) intervals for the mutation-scaled effective immigration rate (M) and mutation-scaled effective population sizes (Θ). Numerals I-V correspond to models in Figure 2. [AM] = Amazonia; [CEPTAF] = Cerrado+Pantanal+Atlantic Forest.

Model	Parameter	Mode	95% HPD
I	Θ	0.00327	0.00240-0.00385
II	$\Theta_{[AM]}$	0.00059	0.00018-0.00107
	$\Theta_{[CEPTAF]}$	0.00348	0.00243-0.00389
	$M_{[AM]\rightarrow[CEPTAF]}$	1667.2	802.7-2891
	$M_{[CEPTAF]\rightarrow[AM]}$	365.2	0-1316
III	$\Theta_{[AM]}$	0.00086	0.00036-0.00147
	$\Theta_{[CEPTAF]}$	0.00345	0.00236-0.00389
	$M_{[AM]\rightarrow[CEPTAF]}$	1368.5	616-2692.7
IV	$\Theta_{[AM]}$	0.00071	0.00011-0.00310
	$\Theta_{[CEPTAF]}$	0.00290	0.00212-0.00372
	$M_{[CEPTAF]\rightarrow[AM]}$	1030.2	289.3-3073
V	$\Theta_{[AM]}$	0.00001	0-0.00025
	$\Theta_{[CEPTAF]}$	0.00295	0.00216-0.00377

CONSIDERAÇÕES FINAIS

A obtenção de uma amostragem representativa da distribuição de uma espécie animal de ampla ocorrência é uma tarefa árdua, a qual ainda é dificultada quando tal espécie apresenta baixas densidades populacionais, sendo incomum de se encontrar e capturar para coleta de tecido. É importante, também, ressaltar a atribuição de alguns indivíduos à Mata Atlântica. Parte das amostras foram coletadas em ecótonos onde o Cerrado adentra áreas cercadas pela Mata Atlântica no Paraná. Portanto, apesar de considerados pertencentes à Mata Atlântica, há a possibilidade de que tais indivíduos sejam oriundos de áreas abertas e estivessem apenas se refugiando ou atravessando áreas de mata. Além disso, a área original da Mata Atlântica foi extensamente transformada pela atividade antrópica, descaracterizando antigas áreas florestadas. Entretanto, apesar das limitações de amostragem inerentes ao estudo apresentado, foram obtidas informações importantes a respeito da estrutura e dinâmica populacional do tamanduá-bandeira, uma espécie ameaçada e pouco estudada do ponto de vista genético.

As principais conclusões deste trabalho são listadas abaixo:

- O DNA mitocondrial indica a existência de dois grupos genéticos moderadamente distintos correspondentes a indivíduos originários da Amazônia (grupo [AM]) e aqueles pertencentes aos biomas Cerrado, Pantanal e Mata Atlântica (grupo [CEPTAF]).
- O tamanduá-bandeira apresenta uma diversidade haplotípica moderada em seu DNA mitocondrial quando comparada a outras espécies ameaçadas e não-ameaçadas.
- A diversidade genética no DNA mitocondrial tende a ser maior em [CEPTAF] do que em [AM], possivelmente, devido a esta última apresentar um menor tamanho populacional.
- Foi detectado um baixo fluxo gênico do grupo [AM] para o [CEPTAF], mas não foi possível descartar sua ausência no sentido contrário. Este resultado pode ser influenciado por maior disponibilidade de alimentos e a preferência por habitats abertos e heterogêneos presentes no Cerrado e Pantanal.
- O tamanho efetivo populacional da espécie aumentou aproximadamente 7.5 vezes nos últimos 60 mil anos, mas as causas ainda não são claras.
- A utilização de sequências nucleares, além de mitocondriais, foi importante para que a análise demográfica pelo método EBSP obtivesse maior precisão nas estimativas de magnitude, data e intervalo de confiança da expansão populacional.